A Noise Analysis for Recovering Reflectances of the Objects Being Imaged

September 2012

Mikiya HIRONAGA

A Noise Analysis for Recovering Reflectances of the Objects Being Imaged

画像入力による分光反射率復元に対するノイズの影響解析

September 2012

Graduate School of Engineering
Osaka City University

Mikiya HIRONAGA
広永　美喜也

Preface

Colors of objects vary under various illuminants. Even under the exact same illuminants, pictures taken by different cameras are not the same because pictures are always under the influence of the illuminants and the sensitivities of the sensors. Thus, recovering the spectral reflectances vector **r** by use of the sensor response vector **p** is important for a reproduction of accurate colors or a stable recognition of colored objects, etc. The sensor response **p** is determined by **p**=SL**r**+**e**, where S is the matrix representing the spectral sensitivities of the image sensors, L is the matrix representing the spectral power distributions of the illuminants and **e** is the additive noise vector. The recovering reflectances **r** from the sensor response **p** is an inverse problem and largely affected by the noise **e**. To recover accurate reflectances by applying a reconstruction matrix W, the study of the noise is required.

Shimano proposed a model estimating the noise variance in an image acquisition device based on the Wiener estimation. He also derived an evaluation model for the quality of an image acquisition device. In this thesis, Shimano's model is examined and extended to an comprehensive model and a robust frame work is proposed for estimating the noise variance and analyzing the effect of the noise to the image acquisition.

This thesis is organized as follows;

In chapter 1, the background and the purpose of the study are briefly described.

In chapter 2, the spectral evaluation model for the image acquisition device based on the Wiener model is examined and the spectral measure of the quality (Qr) of the mage acquisition device for the recovery of the reflectances is studied and it is shown that the Qr can be applied to other reconstruction models with experimental results and mathematical proofs.

In chapter 3, it is shown that the above mentioned model stands in the subspace projected by the sensitivities of the human vision. The colorimetric measure of the quality (Qc) is also applied to multiple reconstruction models and its noise robustness for the quantization error and sampling error is examined Also the concept of the NIF (Noise Influence Factor) is proposed and the reason of the noise sensitivity of an image acquisition device is analyzed.

In chapter 4, the model estimating the noise variance based on the Wiener model is extended and modified to a comprehensive model with a reconstruction matrix W and it is applied to the reconstruction matrices of the Wiener and the linear models. The accuracy of the estimation for the noise variance by the proposed model is confirmed by experiments. The increases in the mean square errors (MSE) of the reconstruction for the reflectances are examined in the Wiener and the linear models and it is shown that the effect of the regularization for the increase in the MSE is well described by the proposed model.

In chapter 5, the overall discussions and conclusions are summarized.

Keywords: spectral reflectances, recovery models, colorimetry, evaluation, spectral discrimination, noise in imaging systems

Contents

List of Figures

List of Tables

Chapter 1

Overall Introduction

This thesis presents a framework for recovering the spectral reflectances of objects being imaged by an image acquisition system. The proposed work estimates and analyzes the noise in the image acquisition device and recovers the reflectances of objects accurately. This chapter addresses the overall introduction of this thesis. The purpose, the background and the sketch of this thesis are also described in this chapter.

The visual information plays an important role for a human being to recognize environments. The visual information mainly consists of shapes and colors. Colors of objects are dependent on the illuminant, the surface of the object, and the sensitivity of the sensors. The illuminant and the sensitivity of the human visual system may vary by circumstances but the spectral reflectances of objects represent the physical properties of objects. Therefore the recovery of spectral reflectances of objects is important not only to reproduce color images under various illuminants [1-3] but also to study computational color vision [4-6] and color constancy [7-9].

Several models have been proposed to recover the spectral reflectances vector **r** by use of the sensor response vector **p** by applying a reconstruction matrix. There are mainly two types of these models, the first is the Wiener estimation, which minimizes the mean square errors (MSEs) between the recovered and the measured spectral reflectances [10-12], and the second is the finite-dimensional linear models of spectral reflectances [13-16]. The spectral sensitivities of the image sensors S, the spectral power distributions of the illuminants L and the learning samples of the spectral reflectances vector **r** which are similar to those of the imaged objects are required for recovering the spectral reflectances by these two models because a sensor response **p** is determined by $\mathbf{p}=SL\mathbf{r}+\mathbf{e}$, where **e** is an additive noise vector. Since it is difficult to measure these spectral characteristics, modifications of these models have been proposed that do not use prior knowledge of the spectral sensitivities of a set of sensors and the spectral power distribution of the illuminant. The modification of the Wiener estimation uses the regression analysis [17] between the known spectral reflectances and the corresponding sensor responses [3,18-22], and this model is called the pseudoinverse transformation or the regression model [18,23]. Another modified linear model also uses the regression analysis between the weight column vectors for the orthonormal basis vectors to represent known spectral reflectances and the corresponding sensor responses [20,24]; in this model the basis vectors are usually derived by the principal

component analysis of spectral the reflectances or derived by singular values decomposition (SVD) [25]. The modified model is called the Imai-Berns model [26,27].

The recovery of the spectral reflectances vector **r** from the sensor response **p** is an inverse problem. Thus, the accuracy of the estimates depends largely on the noise variance used in the Wiener estimation. Recently Shimano proposed a new model to estimate the noise variance of an image acquisition system and also showed that the spectral reflectances of objects being imaged are recovered accurately by using the Wiener estimation through the use of the image data from a multispectral camera without prior knowledge of the spectral reflectance of the objects and the noise present in the image acquisition system [28,29]. He also proposed an evaluation model [30] based on the Wiener estimation to measure the accuracy of the estimation of the reflectances by the image acquisition device.

In multispectral color science, there are two methods for computing characteristics of colors. The one is “spectral” and the other is “colorimetric”. In spectral color processing, every information of color stimulus obtained from the input device is used, on the other hand in colorimetric color processing, color stimuli is divided into two parts, the fundamental and the residual [31]. The fundamental is a projection of a color stimulus onto the human visual subspace (HVSS) spanned by the sensitivities of the cones of the retina and evokes color sensation to a human visual system. The residual is an orthogonal part of the color stimulus and evokes no sensation to a human visual system. The concept for the spectral and the colorimetric is shown in Fig.1.1. Shimano also showed that his model works well both in spectral and colorimetric cases. [32,33] .

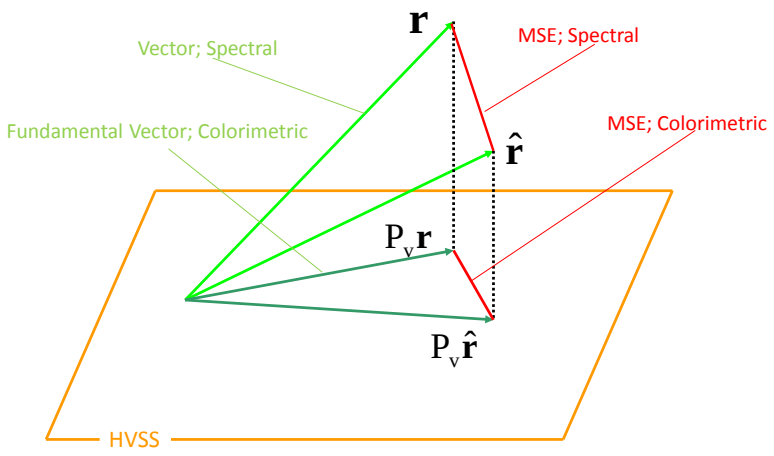

Fig. 1.1. Concepts of spectral and colorimetric; vectors projected onto human visual subspace (HVSS).

This thesis focuses on recovering the reflectances of objects by use of image acquisition devices and on the effect of the noise to the accuracy of the recovery. This thesis addresses that (1) the above mentioned spectral evaluation model based on the Wiener estimation can be applied to other reflectance recovery models, (2) the above mentioned colorimetric evaluation model can be applied to other reflectance recovery models and the evaluation model is noise robust and the model stands in the case as noisy as 20nm sampling interval and 6bit sampling bits and (3) the model to estimate the noise variance of an image acquisition system is extended to a comprehensive model and it is applied not only to the Wiener model but also to the linear model.

This thesis is organized as follows. In chapter 2, the spectral evaluation model for the image acquisition device based on the Wiener model is examined and the spectral measure of the

quality (Qr) of the mage acquisition device for the recovery of the reflectances is studied and it is shown that the Qr can be applied to other reconstruction models with experimental results and mathematical proofs [34]. In chapter 3, it is shown that the above mentioned model stands in the subspace projected by the sensitivities of the human vision (HVSS). The colorimetric measure of the quality (Qc) is also applied to multiple reconstruction models and its noise robustness for the quantization error and sampling error is examined Also the concept of the NIF (Noise Influence Factor) is proposed and the reason of the noise sensitivity is analyzed [35]. In chapter 4, the model estimating the noise variance based on the Wiener model is extended and modified to a comprehensive model with a reconstruction matrix W and it was applied to the reconstruction matrices of the Wiener and the linear models. The accuracy of the estimation for the noise variance by the proposed model is confirmed by experiments. The increases in the mean square errors (MSE) of the reconstruction for the reflectances are examined in the Wiener and the linear models and it is shown that the effect of the regularization for the increase in the MSE is well described by the proposed model. Also the mathematical proof of the equivalence of the proposed model to the existing model in some conditions is described [36]. In chapter 5, the overall discussions and conclusions are summarized.

References

1. M. D. Fairchild, Color Appearance Models (Addison-Wesley, 1997).
2. Y. Miyake and Y. Yokoyama, “Obtaining and reproduction of accurate color images based on human perception,” Proc. SPIE 3300, 190.197 (1998).
3. K. Martinez, J. Cupitt, D. Saunders, and R. Pillay, “Ten years of art imaging research,” Proc. IEEE 90, 28.41 (2002).
4. H. C. Lee, E. J. Breneman, and C. P. Schulte, “Modeling light reflection for computer color vision,” IEEE Trans. Pattern Anal. Mach. Intell. 12, 79.86 (1990).
5. G. Healey and D. Slater, “Global color constancy: recognition of objects by use of illumination-invariant properties of color distributions,” J. Opt. Soc. Am. A 11, 3003.3010 (1994).
6. G. J. Klinker, S. A. Shafer, and T. Kanade, “A physical approach to color image understanding,” Int. J. Comput. Vis. 4, 7.38 (1990).
7. L. T. Maloney and B. A. Wandell, “Color constancy: a method for recovering surface spectral reflectance,” J. Opt. Soc. Am. A 3, 29.33 (1986).
8. J. Ho, B. V. Funt, and M. S. Drew, “Separating a color signal into illumination and surface reflectance components: theory and applications,” IEEE Trans. Pattern Anal. Mach. Intell. 12, 966.977 (1990).
9. G. Iverson and M. D’Zumura, “Criteria for color constancy in trichromatic linear models,” J. Opt. Soc. Am. A 11, 1970.1975 (1994).
10. A. Rosenfeld and A. C. Kak, Digital Picture Processing, 2nd ed. (Academic, 1982).
11. G. Sharma and H. J. Trussell, “Figures of merit for color scanners,” IEEE Trans. Image Process. 6, 990.1001 (1997).
12. H. Haneishi, T. Hasegawa, N. A. Hosoi, Y. Yokoyama, N. Tsumura, and Y. Miyake, “System design for accurately estimating the spectral reflectance of art paintings,” Appl. Opt. 39, 6621.6632 (2000).
13. J. Cohen, “Dependency of spectral reflectance curves of the Munsell color chips,” Psychon. Sci. 1, 369.370 (1964).

14. L. T. Maloney, “Evaluation of linear models of surface spectral reflectance with small numbers of parameters,” J. Opt. Soc. Am. A 3, 1673.1683 (1986).
15. J. P. S. Parkkinen, J. Hallikainen, and T. Jaaskelainen, “Characteristic spectra of Munsell colors,” J. Opt. Soc. Am. A 6, 318.322 (1989).
16. J. L. Dannemiller, “Spectral reflectance of natural objects: how many basis functions are necessary?” J. Opt. Soc. Am. A 9, 507.515 (1992).
17. A. A. Afifi and S. P. Azen, Statistical Analysis, (Academic, 1972), Chap. 3.
18. Y. Zhao, L. A. Taplin, M. Nezamabadi, and R. S. Berns, “Using the matrix R method for spectral image archives,” in Proceedings of The 10th Congress of the International Colour Association(AIC’5) (International Colour Association, 2005), pp. 469.472.
19. H. L. Shen and H. H. Xin, “Spectral characterization of a color scanner based on optimized adaptive estimation,” J. Opt. Soc. Am. A 23, 1566.1569 (2006).
20. D. Connah, J. Y. Hardeberg, and S. Westland, “Comparison of linear spectral reconstruction methods for multispectral imaging,” Proceedings of IEEE’s International Conference on Image Processing (IEEE, 2004), pp. 1497.1500.
21. Y. Zhao, L. A. Taplin, M. Nezamabadi, and R. S. Berns, “Methods of spectral reflectance reconstruction for a Sinarback 54 digital camera,” Munsell Color Science Laboratory Technical Report December 2004, (Munsell Color Science Laboratory, 2004), pp. 1.36.
22. D. Connah and J. Y. Hardeberg, “Spectral recovery using polynomial models,” Proc. SPIE 5667, 65.75 (2005).
23. J. L. Nieves, E. M. Valero, S. M. C. Nascimento, J. H. Andres, and J. Romero, “Multispectral synthesis of daylight using a commercial digital CCD camera,” Appl. Opt. 44, 5696.5703 (2005).
24. F. H. Imai and R. S. Berns, “Spectral estimation using trichromatic digital cameras,” in Proceedings of International Symposium on Multispectral Imaging and Color Reproduction for Digital Archives, (Society of Multispectral Imaging, 1999), pp. 42.49.
25. B. Noble and J. W. Daniel, Applied Linear Algebra, 3rd. ed. (Prentice-Hall, 1988), pp. 338.346.

26. M. A. Lopez-Alvarez, J. Hernandez-Andres, Eva. M. Valero, and J. Romero, “Selecting algorithms, sensors and linear bases for optimum spectral recovery of skylight,” J. Opt. Soc. Am. A 24, 942.956 (2007).
27. V. Cheung, S. Westland, C. Li, J. Hardeberg, and D. Connah, “Characterization of trichromatic color cameras by using a new multispectral imaging technique,” J. Opt. Soc. Am. A 22, 1231.1240 (2005).
28. N. Shimano, “Recovery of spectral reflectances of an art painting without prior knowledge of objects being imaged,” in Proceedings of The 10th Congress of the International Colour Association (International Color Association, 2005), pp. 375.378.
29. N. Shimano, “Recovery of spectral reflectances of objects being imaged without prior knowledge,” IEEE Trans. Image Process. 15, 1848.1856 (2006).
30. N. Shimano, “Evaluation of a multispectral image acquisition system aimed at reconstruction of spectral reflectances”, Opt. Eng. 44, 107115- 1.107115-6 (2005).
31. J. B. Cohen, “Color and color mixture: scalar and vector fundamentals,”Color Res. Appl. 13, 5.39 (1988).
32. N. Shimano, "Suppression of noise effect in color corrections by spectral sensitivities of image sensors," Opt. Rev. 9, 81-88(2002).
33. N. Shimano, "Application of a colorimetric evaluation model to multispectral color image acquisition systems," J. Imaging Sci. Technol. 49, 588-593 (2005).
34. M. Hironaga, N. Shimano, "Evaluating the quality of an image acquisition device aimed at the reconstruction of spectral reflectances using recovery models," J. Imag. Sci. Technol. 52, 030503(2008).
35. M. Hironaga, N. Shimano, "Noise robustness of a colorimetric evaluation model for image acquisition devices with different characterization models," Appl. Opt. 48, 5354-5362 (2009).
36. M. Hironaga and N. Shimano, "Estimating the noise variance in an image acquisition system and its influence on the accuracy of recovered spectral reflectances," Appl. Opt. 49, 6140-6148 (2010).

Chapter 2

Evaluating a quality of an image acquisition device aimed at the reconstruction of spectral reflectances by the use of the recovery models

Accurate recovery of spectral reflectances is important for the color reproduction under a variety of illuminations. To evaluate the quality (Qr) of an image acquisition system aimed at recovery of spectral reflectances, Shimano proposed an evaluation model based on the Wiener estimation [Opt. Eng., **44**, pp.107115-1-6, 2005.] and showed that mean square errors (MSE) between the recovered and measured spectral reflectances as a function of Qr agreed quite well with the prediction by the model.

In this chapter, the evaluation model is applied to two different reflectance recovery models and it is confirmed that the proposed model can be applied to different models with experimental results and mathematical proofs.

2.1 Introduction

Colors are one of the most important characteristics of the human vision and they have been heavily studied to acquire accurate information from color images. The acquisition of the colorimetric information is considered as the acquisition of accurate colorimetric values of objects through the use of sensor responses [1,2]. The accuracy depends on the spectral sensitivities of a set of sensors, the noise present in the acquisition device and the spectral reflectances of the objects etc [1,2]. Therefore the evaluation of the set of sensors is important for the evaluation of the colorimetric performance or optimization of the spectral sensitivities of the sensors. Several models have been proposed to evaluate a colorimetric performance of a set of color sensors [3-7], and the optimization of a set of sensors has been performed based on the evaluation models [8,9]. However, the application of the evaluation models to real color image acquisition devices such as digital cameras and color scanners has not appeared because of the difficulty in estimating noise levels. Recently Shimano proposed a new model to estimate the noise variance of an image acquisition system [10] and applied it to the proposed colorimetric evaluation model and a spectral evaluation model, and confirmed that the evaluation model quite agrees well with the experimental results by multispectral cameras [11].

On the other hand, there is an alternative approach for the color image acquisition. It is the acquisition of the spectral information of the objects being imaged. The purpose of this approach is the acquisition of the spectral reflectances of the imaged objects through the use of sensor responses.[3,12-29]. The acquisition of accurate spectral reflectances of objects is very important in reproducing a color image under a variety of viewing illuminants [30]. The accuracy of the recovered spectral reflectances depends on the number of sensors, their spectral sensitivities, the objects being imaged, the recording illuminants, the noise present in a device and a model used

for the recovery. Therefore the evaluation of a camera aimed at the recovery of spectral reflectances is important for the optimization of an image acquisition system and to get an intuitive understanding about the acquisition of the spectral information. Shimano already derived the evaluation model based on the Wiener estimation [31]. The proposed model is formulated by $\mathrm{MSE}(\sigma^2) = \mathrm{E}_{\max}\left(1 - \mathrm{Q}_{\mathrm{r}}(\sigma^2)\right)$, where $\mathrm{MSE}(\sigma^2)$ is the mean square errors between the recovered and measured spectral reflectances with the estimated noise variance σ^2, Emax represents a constant which is determined only by spectral reflectances of objects and $\mathrm{Qr}(\sigma^2)$ is the quality of the image acquisition system aimed at recovery of spectral reflectances with the estimated noise variance σ^2. It was shown that $\mathrm{Qr}(\sigma^2)$ is determined by the spectral sensitivities of the sensors, the spectral power distribution of the recording illuminant, the noise variance of the image acquisition device and the spectral reflectances of the imaged objects. The model was applied to the multispectral cameras and it was confirmed that the model agrees quite well with the experimental results, i.e., the $\mathrm{MSE}(\sigma^2)$ of the recovered spectral reflectances by the Wiener estimation as a function of the quality $\mathrm{Qr}(\sigma^2)$ of a set of sensors by taking account of the noise shows the straight line. As $\mathrm{Qr}(\sigma^2)$ is derived from Wiener estimation, it is very important to confirm whether the model can be applied to other recovery models since the quality $\mathrm{Qr}(\sigma^2)$ is useful not only for the evaluation of an image acquisition device but also for the optimization of a set of sensors aimed at recovery of spectral reflectances.

In this chapter, it is shown that $\mathrm{Qr}(\sigma^2)$ has a linear relation to the $\mathrm{MSE}(\sigma^2)$ of the reflectances recovered by the multiple regression analysis [18] and the Imai-Berns model [26] by experiments. Mathematical proofs of the equivalence of the Wiener model, the multiple regression model and the Imai-Berns model are given. It is shown that the $\mathrm{Qr}(\sigma^2)$ is also appropriately formulated for these models. Once this linear relation is confirmed, we can estimate $\mathrm{Qr}(\sigma^2)$ by the multiple regression model or the Imai-Berns model, without the spectral

sensitivities of the sensors, spectral power distribution of recording illuminant or estimating the noise variance [32].

This chapter is organized as follows. The outline of the evaluation model and the method to estimate the noise variance and the models tested are briefly reviewed. In the following sections, the experimental procedures and the results to demonstrate the trustworthiness of the proposal are described. The final section presents conclusions and mathematical proofs are in the appendix section.

2.2 Models for the Reconstruction of Spectral Reflectances

In this section, the derivation of the quality $\mathrm{Qr}(\sigma^2)$ to evaluate the color image acquisition system and the models used for the experiments are briefly reviewed.

2.2.1 Wiener Estimation Using Estimated Noise Variance

A vector space notation for color reproduction is useful in the problems. In this approach, the visible wavelengths from 400 to 700 nm are sampled at 10-nm intervals and the number of the samples is denoted as N. A sensor response vector from a set of color sensors for an object with a $\mathrm{N}\times 1$ spectral reflectance vector $\mathbf{r}$ can be expressed by

$$\mathbf{p} = \mathrm{SL}\mathbf{r} + \mathbf{e}, \tag{2.1}$$

where $\mathbf{p}$ is a $\mathrm{M}\times 1$ sensor response vector from the M channel sensors, S is a $\mathrm{M}\times\mathrm{N}$ matrix of the spectral sensitivities of sensors in which a row vector represents a spectral sensitivity, L is an $\mathrm{N}\times\mathrm{N}$ diagonal matrix with samples of the spectral power distribution of an illuminant along the diagonal, and $\mathbf{e}$ is a $\mathrm{M}\times 1$ additive noise vector. The noise $\mathbf{e}$ is defined to include all the sensor response errors such as the measurement errors in the spectral characteristics of sensitivities, an illumination and reflectances, and quantization errors in this work and it is

termed as the system noise[10] below. The system noise is assumed to be signal independent, zero mean and uncorrelated to itself. For abbreviation, let $S_L = SL$. The mean square errors (MSE) of the recovered spectral reflectances $\hat{\mathbf{r}}$ is given by

$$\mathrm{MSE} = \mathrm{E}\left\{\left\|\mathbf{r} - \hat{\mathbf{r}}\right\|^2\right\}, \tag{2.2}$$

where $\mathrm{E}\{\bullet\}$ represents the expectation. If $\hat{\mathbf{r}}$ is given by $\hat{\mathbf{r}} = W_0\mathbf{p}$, the matrix W_0 which minimizes the MSE is given by

$$W_0 = \mathrm{Rss}S_L^T\left(S_L\mathrm{Rss}S_L^T + \sigma_e^2\mathrm{I}\right)^{-1}, \tag{2.3}$$

where T represents the transpose of a matrix, Rss is an autocorrelation matrix of the spectral reflectances of samples that will be captured by a device, and σ_e^2 is the noise variance used for the estimation. Substitution of Eq.(2.3) into Eq.(2.2) leads to [10]

$$\mathrm{MSE}(\sigma_e^2) = \sum_{i=1}^{N}\lambda_i - \sum_{i=1}^{N}\sum_{j=1}^{\beta}\lambda_i b_{ij}^2 + \sum_{i=1}^{N}\sum_{j=1}^{\beta}\frac{\sigma_e^4 + \kappa_j^{v\,2}\sigma^2}{\left(\kappa_j^{v\,2} + \sigma_e^2\right)^2}\lambda_i b_{ij}^2, \tag{2.4}$$

where λ_i is the eigenvalues of Rss, b_{ij}, κ_j^v and β represent i-th row of the j-th right singular vector, singular value and a rank of a matrix $S_L V\Lambda^{1/2}$, respectively, σ^2 is the actual system noise variance, V is a basis matrix and Λ is an $N \times N$ diagonal matrix with positive eigenvalues λ_i along the diagonal in decreasing order. It is easily seen that the MSE is minimized when $\sigma_e^2 = \sigma^2$, and the $\mathrm{MSE}(\sigma^2)$ is given by

$$\mathrm{MSE}(\sigma^2) = \sum_{i=1}^{N}\lambda_i - \sum_{i=1}^{N}\sum_{j=1}^{\beta}\lambda_i b_{ij}^2 + \sum_{i=1}^{N}\sum_{j=1}^{\beta}\frac{\sigma^2}{\kappa_j^{v\,2} + \sigma^2}\lambda_i b_{ij}^2 . \tag{2.5}$$

Equation (2.5) can be rewritten as

$$\mathrm{MSE}(\sigma^2) = \sum_{i=1}^{N} \lambda_i \left(1 - \frac{\Sigma_{i=1}^{N} \Sigma_{j=1}^{\beta} \lambda_i b_{ij}^2 - \Sigma_{i=1}^{N} \Sigma_{j=1}^{\beta} \dfrac{\sigma^2}{\kappa_j^{v^2} + \sigma^2} \lambda_i b_{ij}^2}{\Sigma_{i=1}^{N} \lambda_i} \right). \tag{2.6}$$

Therefore the quality of a set of color sensors in the presence of noise is formulated as

$$Q_r(\sigma^2) = \frac{\Sigma_{i=1}^{N} \Sigma_{j=1}^{\beta} \lambda_i b_{ij}^2 - \Sigma_{i=1}^{N} \Sigma_{j=1}^{\beta} \dfrac{\sigma^2}{\kappa_j^{v^2} + \sigma^2} \lambda_i b_{ij}^2}{\Sigma_{i=1}^{N} \lambda_i}. \tag{2.7}$$

Hence, the $\mathrm{MSE}(\sigma^2)$ is expressed as

$$\mathrm{MSE}(\sigma^2) = E_{\max}\left(1 - Q_r(\sigma^2)\right), \tag{2.8}$$

where $E_{\max} = \sum_{i=1}^{N} \lambda_i$. This equation shows that the $\mathrm{MSE}(\sigma^2)$ has a linear relation to $\mathrm{Qr}(\sigma^2)$ and the slope of the line is $\sum_{i=1}^{N} \lambda_i$. The values of $\sum_{i=1}^{N} \lambda_i$ are dependent only on the surface spectral reflectance of the objects being captured. The $\mathrm{MSE}(\sigma^2)$ decreases as the $\mathrm{Qr}(\sigma^2)$ increases to one.

If we let the noise variance $\sigma_e^2 = 0$ for the Wiener filter in Eq. (2.3), then the $\mathrm{MSE}(0)$ is derived as (by letting $\sigma_e^2 = 0$ in Eq. (2.4))

$$\mathrm{MSE}(0) = \sum_{i=1}^{N} \lambda_i - \sum_{i=1}^{N} \sum_{j=1}^{\beta} \lambda_i b_{ij}^2 + \sum_{i=1}^{N} \sum_{j=1}^{\beta} \frac{\sigma^2}{\kappa_j^{v^2}} \lambda_i b_{ij}^2. \tag{2.9}$$

The first and second terms on the right-hand side of Eq. (2.9) represent the $\mathrm{MSE}(0)$ at a noiseless case. We denote this MSE as $\mathrm{MSE}_{\mathrm{free}}$, then the estimated system noise variance $\hat{\sigma}^2$ can be represented by

$$\hat{\sigma}^2 = \frac{\mathrm{MSE}(0) - \mathrm{MSE}_{\mathrm{free}}}{\Sigma_{i=1}^{N}\Sigma_{j=1}^{\beta}\dfrac{\lambda_i b_{ij}^2}{\kappa_j^{v^2}}}, \tag{2.10}$$

where $\mathrm{MSE}_{\mathrm{free}}$ is given by

$$\mathrm{MSE}_{\mathrm{free}} = \sum_{i=1}^{N}\lambda_i - \sum_{i=1}^{N}\sum_{j=1}^{\beta}\lambda_i b_{ij}^2. \tag{2.11}$$

Therefore, the system noise variance σ^2 can be estimated using Eq. (2.10), since the $\mathrm{MSE}_{\mathrm{free}}$ and the denominator of Eq. (2.10) can be computed if the surface reflectance spectra of objects, the spectral sensitivities of sensors and the spectral power distribution of an illuminant are known. The $\mathrm{MSE}(0)$ can also be obtained by the experiment using Eqs. (2.2) and (2.3) applying the Wiener filter with $\sigma_e^2 = 0$ to sensor responses. Therefore, Eq. (2.10) gives a method to estimate the actual noise variance σ^2. [10]

The quality $\mathrm{Qr}(\sigma^2)$ and $\mathrm{MSE}(\sigma^2)$ can be computed by substituting the estimated noise variance in Eq.(2.7) and Eq.(2.3) , respectively.

2.2.2 Multiple Regression Analysis

Let $\mathbf{p}_i$ be a $M \times 1$ sensor response vector which is obtained by the image acquisition of a known spectral reflectance $\mathbf{r}_i$ of the i-th object, where i represents a number. Let P be a $M \times k$ matrix which contains the sensor responses $\mathbf{p}_1, \mathbf{p}_2, \cdots, \mathbf{p}_k$, and let R be a $N \times k$ matrix which contains the corresponding spectral reflectances $\mathbf{r}_1, \mathbf{r}_2, \cdots, \mathbf{r}_k$, where k is the number of the learning samples. The pseudoinverse model is to find a matrix W which minimizes $\|R - WP\|$, where notation $\|\bullet\|$ represents the Frobenius norm[33]. The matrix W is given by.

$$W = RP^{+}, \tag{2.12}$$

where P^+ represents the pseudo inverse matrix of the matrix P. By applying a matrix W to a sensor response vector $\mathbf{p}$, i.e., $\hat{\mathbf{r}} = W\mathbf{p}$, a spectral reflectance is estimated. Therefore this model does not use the spectral sensitivities of sensors or the spectral power distribution of an illumination, but it uses only the spectral reflectances of the learning samples.

2.2.3 Imai-Berns Model

The Imai-Berns model [26] is considered as the modification of the linear model by using the multiple regression analysis between the weight column vectors for basis vectors to represent the known spectral reflectances and corresponding sensor response vectors.

Let Σ be a $d \times k$ matrix which contains the column vectors of the weights $\boldsymbol{\sigma}_1, \boldsymbol{\sigma}_2, \cdots, \boldsymbol{\sigma}_k$ to represent the k known spectral reflectances $\mathbf{r}_1, \mathbf{r}_2, \cdots, \mathbf{r}_k$ and let P be a $M \times k$ matrix which contains corresponding sensor response vectors of those reflectances $\mathbf{p}_1, \mathbf{p}_2, \cdots, \mathbf{p}_k$,where d is a number of the weights to represent the spectral reflectances. The multiple regression analysis between these matrixes is expressed as $\|\Sigma - BP\|$. A matrix B which minimize the Frobenius norm is given by

$$B = \Sigma P^+ . \tag{2.13}$$

Since a weight column vectors $\boldsymbol{\sigma}$ for a sensor response vector $\mathbf{p}$ is estimated by $\hat{\boldsymbol{\sigma}} = B\mathbf{p}$, the estimated spectral reflectance vector is derived from $\hat{\mathbf{r}} = \mathbf{V}\hat{\boldsymbol{\sigma}}$, where a matrix V is the basis matrix which contains first d orthonormal basis vectors of spectral reflectances. This model does not use the spectral characteristics of sensors or an illumination.

2.3 Experimental Procedures

A multispectral color image acquisition system was assembled by using seven interference filters (Asahi Spectral Corporation) in conjunction with a monochrome video camera (Kodak

KAI-4021M). Image data from the video camera were converted to 16-bit-depth digital data by an AD converter. The spectral sensitivity of the video camera was measured over wavelength from 400 to 700 nm at 10-nm intervals. The measured spectral sensitivities of the camera with each filter are shown in Fig.2.1. The illuminant used for image capture was the illuminant which simulates daylight (Seric Solax XC-100AF). The spectral power distribution of the illuminant measured by the spectroradiometer (Minolta CS-1000) is presented in Fig.2.2.

The GretagMacbeth ColorChecker (24 colors) and the Kodak Q60R1 (228 Colors), let us denote them CC and KK respectively for abbreviation, were illuminated from the direction of about 45 degree to the surface normal, and the images were captured by the camera from the normal direction. The image data were corrected to uniform the nonuniformity in illumination and sensitivities of the pixels of a CCD. The computed responses from a camera to a color by using the measured spectral sensitivities of the sensors, the illuminant and the surface reflectance of the color dose not equal to the actual sensor responses since the absolute spectral sensitivities of a camera depend on the camera gain. Therefore, the sensitivities were calibrated using an achromatic color in the charts. In this work, the constraint is imposed on the signal power as given by $\rho = \mathrm{Tr}\left(S_L R_{SS} S_L^T\right)$, where relation of $\rho = 1$ was used so that the estimated system noise variance can be compared for different sensor sets.

By using various combinations of sensors from the three to seven in Fig.2.1, the system noise variance was estimated by the methods described above for each combination of sensors. Then the estimated noise variance was used to recover the spectral reflectances by the Wiener estimation, and then the MSE (σ^2) of the recovered spectral reflectances was computed. The spectral reflectances were also recovered by the multiple regression model and the Imai-Berns model. By using the estimated noise variance, the quality Qr (σ^2) for each combination of sensors was computed using Eq.(2.7).

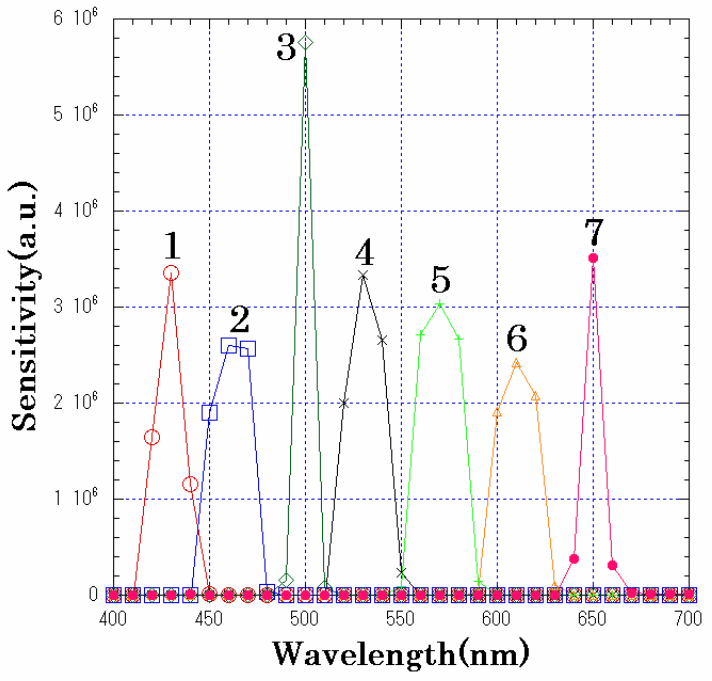

Fig. 2.1. Spectral sensitivities of the sensors of the camera.

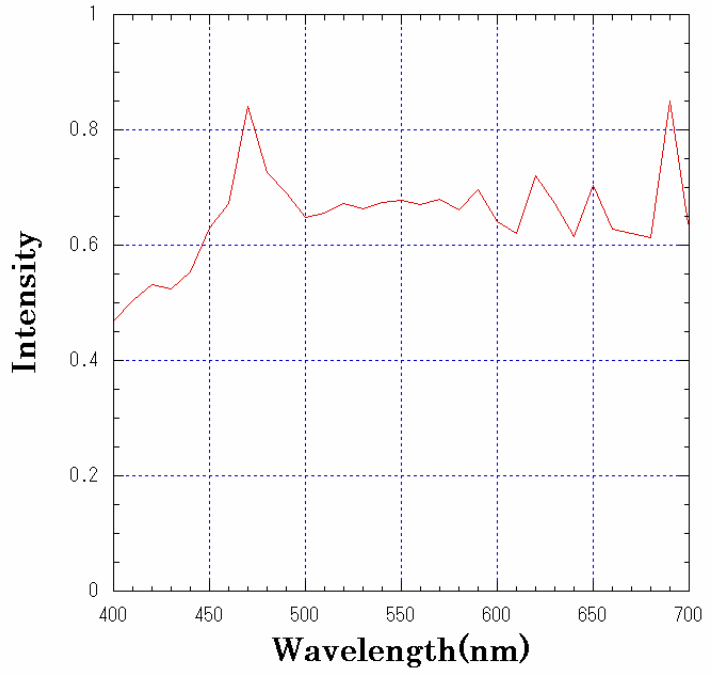

Fig. 2.2. Spectral power distribution of the illumination.

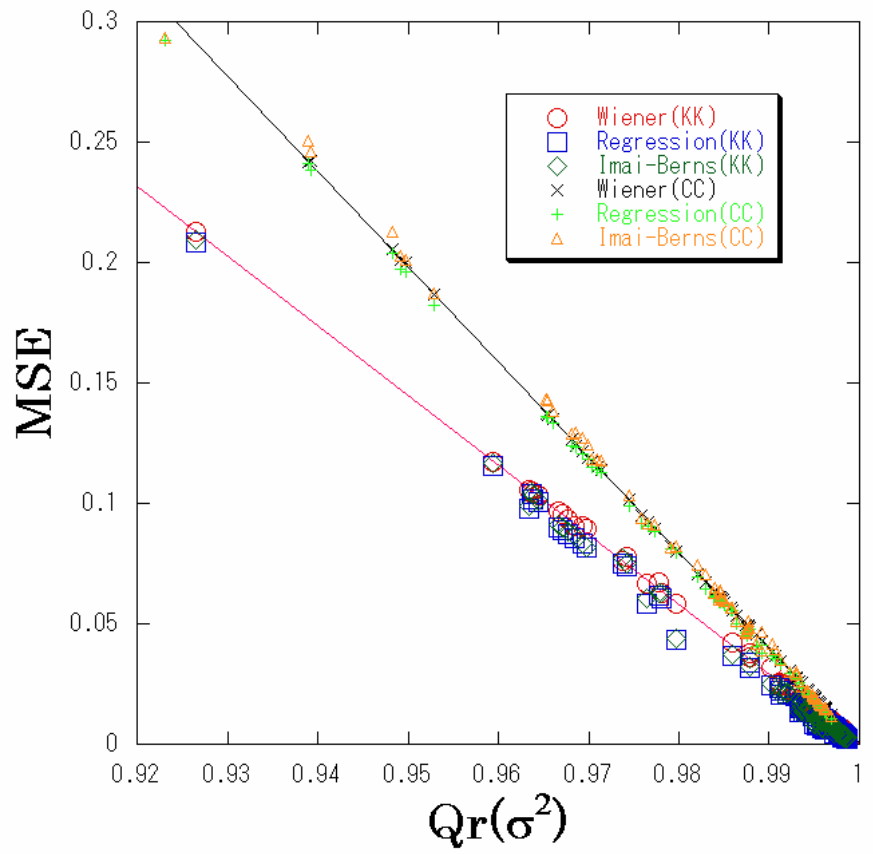

Fig. 2.3. MSEs of the recovered spectral reflectances by the Wiener, Regression, and Imai-Berns method for the GretagMacbeth ColorChecker (CC) and the Kodak Q60R1 (KK) are plotted as a function of $\mathrm{Qr}(\sigma^2)$.

2.4 Results and Discussions

The values of the $\mathrm{MSE}(\sigma^2)$ of the CC and KK as a function of $\mathrm{Qr}(\sigma^2)$ for the 80 sets of sensors are shown in Fig.2.3. The lines in the figure indicate the theoretical relation between the $\mathrm{MSE}(\sigma^2)$ and $\mathrm{Qr}(\sigma^2)$ as given by Eq. (2.8) for two color charts, where $E_{max} = \sum_{i=1}^{N} \lambda_i$ was used for the determination of the slopes of the line for each color chart. The experimental results of the MSE as a function of $\mathrm{Qr}(\sigma^2)$ by the multiple regression analysis and the Imai-Berns method agree well with the theoretical lines.

To show the importance of considering the noise variance, let $Qr(0)$ be the value of $Qr(\sigma^2)$ when the noise variance $\sigma^2 = 0$, i.e.,

$$Q_r(0) = \frac{\Sigma_{i=1}^{N}\Sigma_{j=1}^{\beta}\lambda_i b_{ij}^2}{\Sigma_{i=1}^{N}\lambda_i}. \tag{2.14}$$

Note that the Eq. (2.9) was used as the MSEs of the recovered reflectances by the Wiener filter with zero noise variance. The relation between MSE and $Qr(0)$ is shown in Fig.2.4.

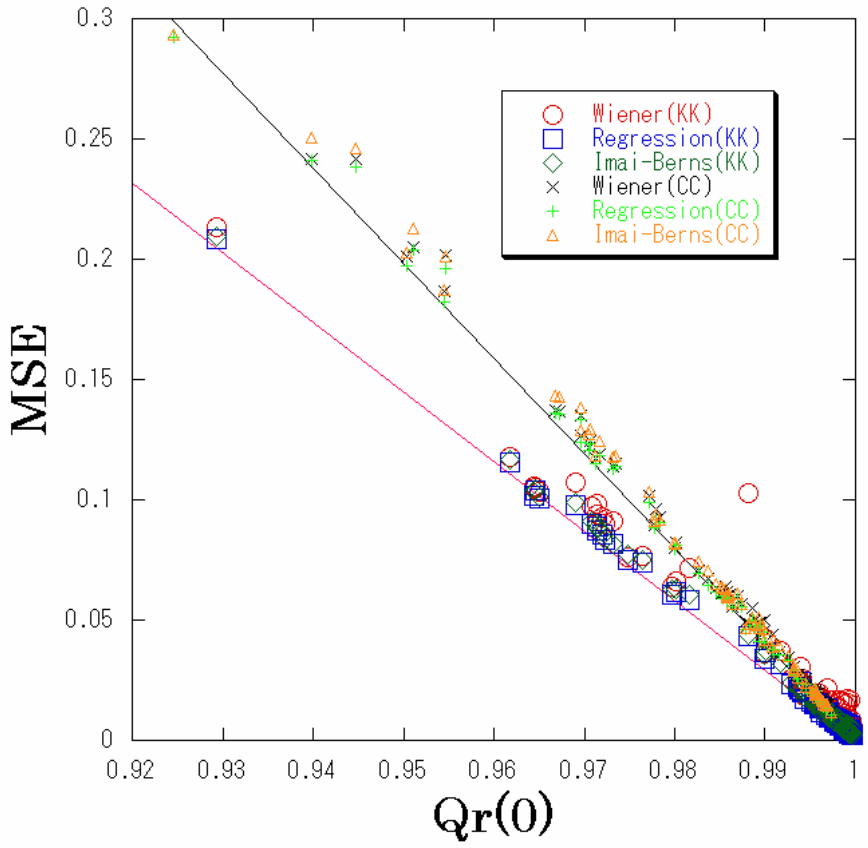

Fig. 2.4. MSEs of the recovered spectral reflectances by the Wiener, Regression, and Imai-Berns method for the GretagMacbeth ColorChecker (CC) and the Kodak Q60R1 (KK) are plotted as a function of $Qr(0)$, which is the value of $Qr(\sigma^2)$ when the estimated noise variance is zero. This is the case without consideration for the noise.

In Fig.2.4 plots not only disagree with the theoretical lines but also scatter more largely compared to the Fig.2.3. Especially the plots of the KK recovered by the Wiener model scatter far above the theoretical line. These scattered plots indicate the importance of the accurate estimation of the noise variance in the images. Also we confirmed that plots of the CC scatter more largely in Fig.2.4 when the 6-bit AD converter is used instead of the 16-bit converter to digitize the sensor responses.

The results in Fig.2.3 agree well with the theoretical predictions and it means that $\mathrm{Qr}(\sigma^2)$ is able to be used for the multiple regression analysis and the Imai-Berns model. As a matter of a fact, the multiple regression model and the Imai-Berns model are mathematically equivalent to the Wiener estimation, i.e., the matrixes W in Eq.(2.12) and B in Eq. (2.13) are equivalent to the matrix of the Wiener filter W_0 in Eq.(2.3) and which can be proved by the mathematical analysis. For proofs of the equivalences, see the appendix.

Typical examples of the recovered reflectances and the reproduced color images for three cases of the $\mathrm{Qr}(\sigma^2)$ are shown in Fig.2.5 through Fig.2.7. It is very clear that the error of the recovered spectral reflectances increase with a decrease in the $\mathrm{Qr}(\sigma^2)$ and faithfulness of the reproduced colors decreases with a decrease in the $\mathrm{Qr}(\sigma^2)$. Also the typical examples of the maximum and minimum values of the $\mathrm{Qr}(\sigma^2)$ and $\mathrm{MSE}(\sigma^2)$ by the three models for each number (three to seven) of sensor sets are shown in Table 2.1. It is very interesting that a set of four sensors (sensor number “2457”) has a larger $\mathrm{Qr}(\sigma^2)$ than a set of six sensors (sensor number “123456”). It is not always true that the $\mathrm{Qr}(\sigma^2)$ increases when the number of the sensors increases.

Though we confirmed that the Wiener model recovers the reflectances most accurately of the three reflectance recovery models such as the Wiener, the regression and the Imai-Berns model in most cases, especially in the cases when the reflectances of the learning sample and the test

sample are not similar [34] and that the Wiener model recovers the highly accurate reflectances by selecting the appropriate learning samples from a group of samples or databases of reflectances of objects [35], we have to recover the reflectances by the multiple regression model or the Imai-Berns model when prior knowledge of the spectral sensitivities of a set of sensors or the spectral power distribution of the illuminant are unknown. In other words, we have to evaluate the image acquisition devices by the multiple regression model or the Imai-Berns model when prior knowledge of the image acquisition device is unknown. It is now confirmed that the MSE (σ^2) of the spectral reflectances recovered by the multiple regression model and the Imai-Berns model have a linear relation to the quality Qr (σ^2) of the image acquisition system. Once this linear relation is confirmed, we can estimate Qr (σ^2) by the multiple regression or the Imai-Berns model without the spectral sensitivities of sensors, the spectral power distribution of the recording illuminant or the noise present in the image acquisition system since it (Qr (σ^2)) can be easily estimated by marking the value of the MSE by the models on the theoretical line, i.e., the corresponding Qr (σ^2) of the point gives the estimate.

Now it is possible to estimate the quality Qr (σ^2) by the multiple regression model or the Imai-Berns model with only the spectral reflectances and the captured images of the object.

2.5 Conclusions

The evaluation of an image acquisition system aimed at recovery of spectral reflectances, which is derived based on the Wiener estimation, was applied to the multiple regression analysis and the Imai-Berns method. The experimental results by multispectral cameras agree quite well with the proposed model. From this result, it is concluded that the proposed evaluation model is appropriately formulated and that the estimation of the noise variance of an image acquisition system is essential to evaluate the quality Qr (σ^2). This result also gives us an easy way to

estimate the quality $Qr(\sigma^2)$ and provides us an easier way to evaluate an image acquisition system aimed at reconstruction of spectral reflectances without the spectral sensitivities of sensors, the spectral power distribution of the recording illuminant or the noise present in the image acquisition system [36].

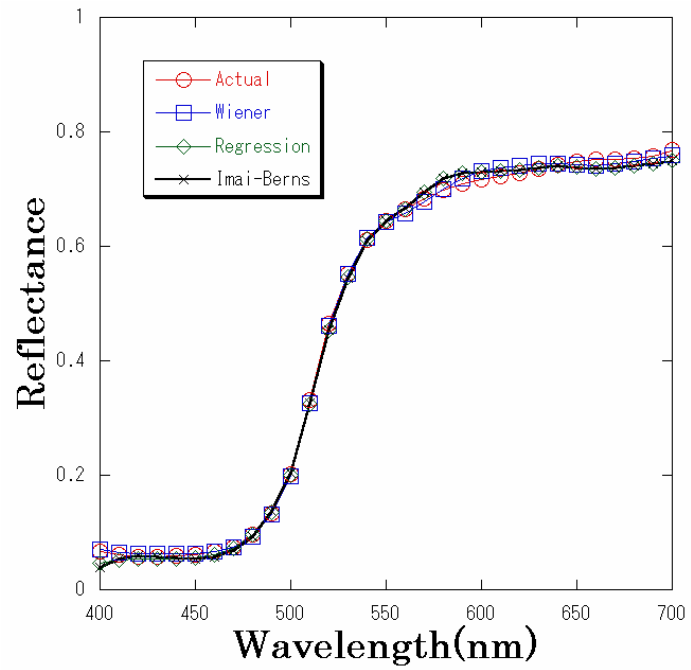

(a)

(b)

Fig. 2.5. (a) Typical example of the recovered spectral reflectance of the color red at a large $Qr(\sigma^2)$ ($Qr(\sigma^2)$ = 0.996894). (b) Color reproduction of the GretagMacbeth ColorChecker by the recovered spectral reflectance at $Qr(\sigma^2)$ = 0.996894.

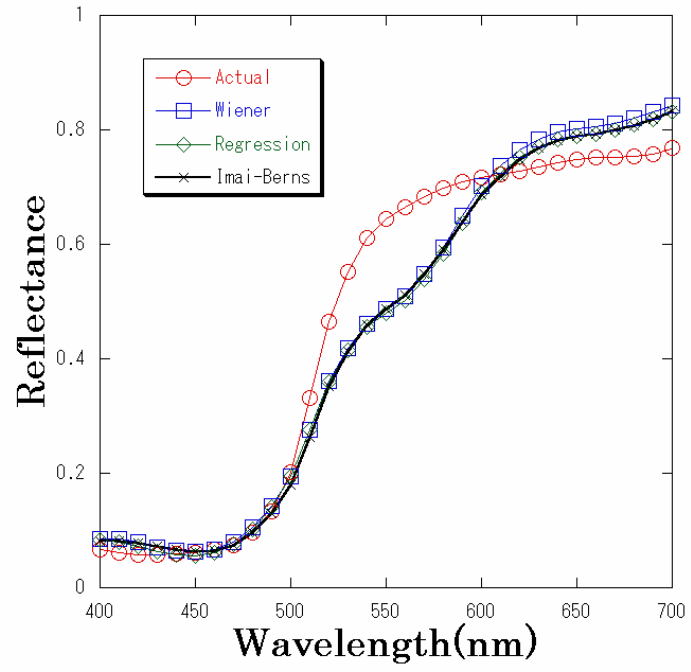

(a)

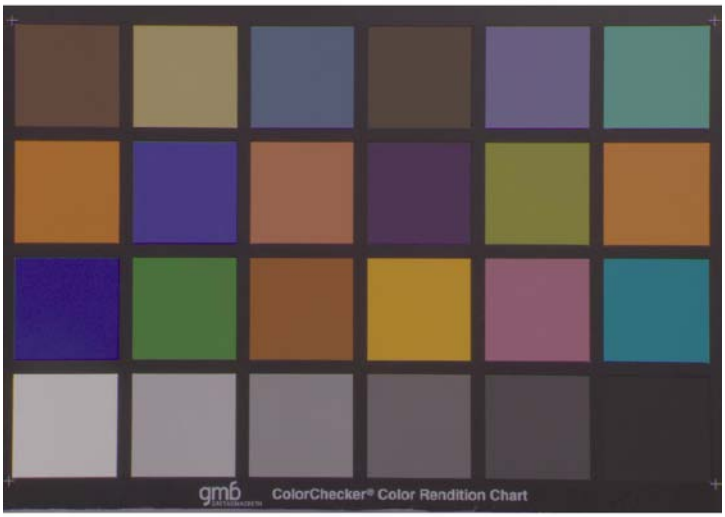

(b)

Fig. 2.6. (a) Typical example of the recovered spectral reflectance of the color red at a middle $Qr(\sigma^2)$ ($Qr(\sigma^2)$ = 0.965348). (b) Color reproduction of the GretagMacbeth ColorChecker by the recovered spectral reflectance at $Qr(\sigma^2)$ = 0.965348.

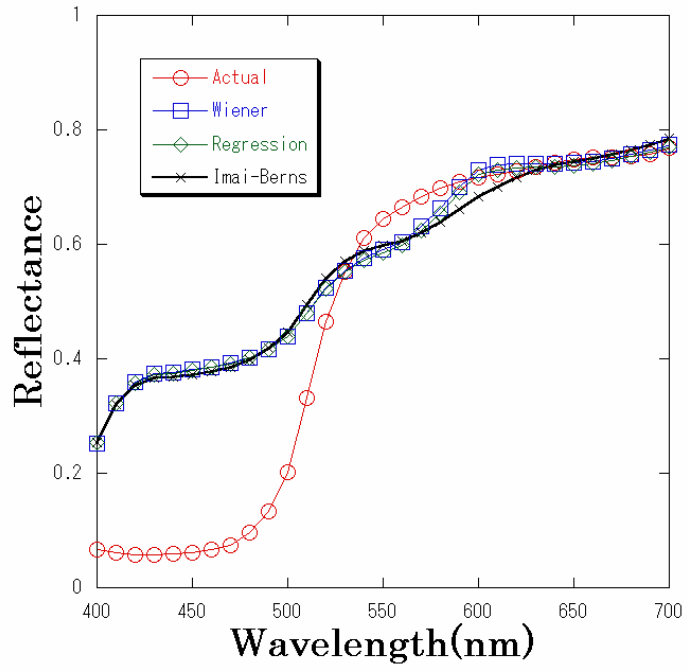

(a)

(b)

Fig. 2.7. (a) Typical example of the recovered spectral reflectance of the color red at a small $Qr(\sigma^2)$ ($Qr(\sigma^2)$ = 0.938896). (b) Color reproduction of the GretagMacbeth ColorChecker by the recovered spectral reflectance at $Qr(\sigma^2)$ = 0.938896.

Table 2.1. Maximum and minimum $Qr(\sigma^2)$ for each number of sensors of the Macbeth ColorChecker.

$Qr(\sigma^2)$	Number of sensors	Sensors	Qr(0)	$MSE(\sigma^2)$ (Wiener)	MSE(0)	MSE (Regression)	MSE (Imai-Berns)
0.996894	7ch	1234567	0.997397	0.012164	0.012423	0.010682	0.011500
0.996324	6ch	134567	0.996891	0.014354	0.014631	0.013326	0.014258
0.995627	5ch	13467	0.996312	0.017177	0.017348	0.016063	0.016816
0.993334	4ch	2457	0.993690	0.026408	0.026374	0.025583	0.026071
0.989134	6ch	123456	0.990872	0.043106	0.043771	0.037802	0.038943
0.987814	3ch	257	0.988318	0.048248	0.048213	0.047758	0.048249
0.923114	5ch	12345	0.924614	0.304426	0.304508	0.292043	0.293503
0.856650	4ch	1234	0.860630	0.569539	0.569701	0.558052	0.563130
0.787850	3ch	123	0.791501	0.838561	0.839893	0.817497	0.826465

References

1. P.S. Hung, “Colorimetric calibration for scanners and media,” Proc. SPIE **1448**, 164-174 (1991).
2. H.R. Kang, “Colorimetric scanner calibration”, J. Imaging Sci. Technol. **36**(2), 162-170 (1992).
3. G. Sharma and H.J. Trussell, “Figure of merit for color scanners,” IEEE Trans. Image Process. **6**(7), 990-1001 (1997).
4. N. Shimano, “Suppression of noise effect in color corrections by spectral sensitivities of image sensors,” Opt. Rev. **9**(2), 81-88 (2002).
5. S. Quan, N. Ohta, R.S. Berns, X. Jiang and N. Katoh, “Unified measure of goodness and optimal design of spectral sensitivity functions,” J. Imaging Sci. Technol. **46**(6), 485-497 (2002).
6. H.E.J. Neugebauer “Quality factor for filters whose spectral transmittances are different from color mixture curves, and its application to color photography.” J. Opt. Soc. Am. **46**(10),821-824 (1956)
7. P.L. Vora and H.J. Trussell, “Measure of goodness of a set of color-scanning filters,” J. Opt. Soc. Am. A **10**(7), 1499-1508 (1993).
8. N. Shimano, "Optimization of spectral sensitivities with Gaussian distribution functions for a color image acquisition device in the presence of noise", Optical Engineering, vol.**45**(1)., pp.013201-1-8, (2006).
9. G. Sharma, H.J. Trussell and M.J. Vrhel, “Optimal nonnegative color scanning filters,” IEEE Trans Image Process. **7**(1), 129-133 (1998).
10. N. Shimano, "Recovery of Spectral Reflectances of Objects Being Imaged Without Prior Knowledge" IEEE Trans. Image Process. vol. **15**, no.7, pp. 1848-1856, Jul. (2006).
11. N. Shimano, “Application of a Colorimetric Evaluation Model to Multispectral Color Image Acquisition Systems” J. Imaging Sci. Technol. **49**(6), 588-593 (2005).
12. J. Cohen, "Dependency of spectral reflectance curves of the Munsell color chips", Psychon. Sci, **1**, 369-370(1964).

13. L. T. Maloney, "Evaluation of linear models of surface spectral reflectance with small numbers of parameters", J. Opt. Soc. Am. A**3**, 1673-1683(1986).
14. J. P. S. Parkkinen, J. Hallikainen, T. Jaaskelainen, "Characteristic Spectra of Munsell Colors", J. Opt. Soc. Am. A**6**, 318-322(1989).
15. J. L. Dannemiller, "Spectral reflectance of natural objects: how many basis functions are necessary?" J. Opt. Soc. Am. A**9**, 507-515(1992).
16. A. Rosenfeld and A. C. Kak, Digital Picture Processing, 2nd ed., (Academic Press, 1982).
17. H. Haneishi, T. Hasegawa, N. A. Hosoi, Y. Yokoyama, N. Tsumura and Y. Miyake, "System design for accurately estimating the spectral reflectance of art paintings", Appl. Optics, **39**,6621-6632(2000).
18. Y. Zhao, L.A. Taplin, M. Nezamabadi and R.S. Berns, “Using the Matrix R Method for Spectral Image Archives”, The 10th Congress of the International Color Association (AIC’5), (Granada, Spain), pp.469-472 (2005).
19. K. Martinez, J. Cupitt, D. Saunders and R. Pillay, "Ten Years of Art Imaging Research", Proc. of the IEEE, **90**,28-41(2002).
20. A. A. Afifi and S. P. Azen, "Statistical Analysis", Chap.3,(Academic Press,1972).
21. H. L. Shen and H. H. Xin, "Spectral characterization of a color scanner based on optimized adaptive estimation", J. Opt. Soc. Am. A**23**, 1566-1569(2006).
22. D. Connah, J. Y. Hardeberg, and S. Westland, "Comparison of Linear Spectral Reconstruction Methods for Multispectral Imaging", Proc. IEEE's International Conference on image Processing (IEEE,2004),pp.1497-1500.
23. Y. Zhao, L. A. Taplin, M. Nezamabadi, and R. S. Berns, "Methods of Spectral Reflectance Reconstruction for A Sinarback 54 Digital Camera", Munsell Color Science Laboratory Technical Report December 2004,pp.1-36(2004).
24. D. Connah and J. Y. Hardeberg, "Spectral recovery using polynomial models” Proc. SPIE **5667**, 65-75 (2005)
25. J. L. Nieves, E. M. Valero, S. M. C. Nascimento, J. H. Andrés, and J. Romero, "Multispectral synthesis of daylight using a commercial digital CCD camera", Appl. Optics, **44**, 5696-5703(2005).

26. F.H. Imai and R.S. Berns, "Spectral Estimation Using Trichromatic Digital Cameras", Proc. Int. Symposium on Multispectral Imaging and Color Reproduction for Digital Archives, Chiba, Japan. 42-49, (1999).
27. M. A. López-Álvarez, J. Hernández-Andrés, Eva. M. Valero and J. Romero, "Selecting algorithms, sensors and liner bases for optimum spectral recovery of skylight" J. Opt. Soc. Am. A**24**,942-956(2007).
28. V. Cheung, S. Westland, C. Li, J. Hardeberg and D. Connah, "Characterization of trichromatic color cameras by using a new multispectral imaging technique", J. Opt. Soc. Am. A**22**, 1231-1240(2005).
29. M. Shi and G. Healey, “Using reflectance models for color scanner calibration”, J. Opt. Soc. Am. A **19**(4), 645-656 (2002).
30. Y. Miyake and Y. Yokoyama, "Obtaining and Reproduction of Accurate Color Images Based on Human Perception", Proc. SPIE **3300**, 190-197(1998).
31. N. Shimano, "Evaluation of a multispectral image acquisition system aimed at reconstruction of spectral reflectances", Optical Engineering, vol.**44**, pp.107115-1-6, (2005).
32. M. Hironaga, K. Terai and N. Shimano, “A model to evaluate color image acquisition systems aimed at the reconstruction of spectral reflectances”, Proc. Ninth International Symposium on Multispectral Color Science and Application, Taipei, R.O.C. 23-28, (2007).
33. G.H. Golub and C.F.V. Loan, "Matrix Computations", The Johns Hopkins
34. N. Shimano, K. Terai, and M. Hironaga, "Recovery of spectral reflectances of objects being imaged by multispectral cameras," J. Opt. Soc. Am. A 24, 3211-3219 (2007).
35. N. Shimano and M. Hironaga, "Recovery of spectral reflectances of imaged objects by the use of features of spectral reflectances," J. Opt. Soc. Am. A 27, 251-258 (2010).
36. M. Hironaga, N. Shimano, "Evaluating the quality of an image acquisition device aimed at the reconstruction of spectral reflectances using recovery models," J. Imag. Sci. Technol. 52, 030503(2008).

Appendix

A. Proof of the equivalence of the multiple regression model to the Wiener model.

The multiple regression model minimizes

$$\left\| \mathrm{R} - \mathrm{WP} \right\|, \tag{A2.1}$$

where P is a $\mathrm{M} \times \mathrm{k}$ matrix which contains the sensor response vectors $\mathbf{p}_1, \mathbf{p}_2, \cdots, \mathbf{p}_\mathrm{k}$ and let R be a $\mathrm{N} \times \mathrm{k}$ matrix which contains the corresponding spectral reflectances vectors $\mathbf{r}_1, \mathbf{r}_2, \cdots, \mathbf{r}_\mathrm{k}$, where k is the number of the learning samples. The $\mathrm{N} \times \mathrm{M}$ matrix W which minimizes Eq.(A2.1) is given by

$$\mathrm{W} = \mathrm{RP}^{+}, \tag{A2.2}$$

where P^{+} represents the pseudo inverse matrix of the matrix P.

$$\mathrm{P}^{+} = \mathrm{P}^{\mathrm{T}} (\mathrm{PP}^{\mathrm{T}})^{-1} \tag{A2.3}$$

because $\mathrm{M} < \mathrm{k}$ holds in the image acquisition devices and $\mathrm{Rank(P)} = \mathrm{M}$. Let

$$\mathrm{P} = \mathrm{SLR} + \mathrm{E}, \tag{A2.4}$$

where S is a $\mathrm{M} \times \mathrm{N}$ matrix of the spectral sensitivities of sensors in which a row vector represents a spectral sensitivity, L is an $\mathrm{N} \times \mathrm{N}$ diagonal matrix with samples of the spectral power distribution of an illuminant along the diagonal, and E is a $\mathrm{M} \times \mathrm{N}$ matrix which contains the additive noise vectors. For abbreviation, let $\mathrm{S}_\mathrm{L} = \mathrm{SL}$. Substitution of Eq. (A2.3) and Eq. (A2.4) into Eq. (A2.2) leads to

$$\mathrm{W} = \mathrm{R}(\mathrm{S}_\mathrm{L}\mathrm{R} + \mathrm{E})^{\mathrm{T}} ((\mathrm{S}_\mathrm{L}\mathrm{R} + \mathrm{E})(\mathrm{S}_\mathrm{L}\mathrm{R} + \mathrm{E})^{\mathrm{T}})^{-1}. \tag{A2.5}$$

Hence W is rewritten as

$$W = RssS_L^T\left(S_L RssS_L^T + \sigma_e^2 I\right)^{-1} \tag{A2.6}$$

because RR^t is an autocorrelation matrix of R and EE^t gives the noise variance and $RE^T = ER^T = 0$ as the spectral reflectances and the error have no correlation.

Thus the matrix W is equivalent to that of the Wiener filter.

B. Proof of the equivalence of the Imai-Berns model to the Wiener model.

Let Σ be a $d \times k$ matrix which contains the vectors of the weights to represent the k known spectral reflectances, where d is a number of the weights to represent the spectral reflectances and let P, R, S_L and E be as defined in Appendix A.

A $d \times M$ matrix B which minimizes

$$\left\|\Sigma = BP\right\| \tag{B2.1}$$

is given by

$$B = \Sigma P^+ . \tag{B2.2}$$

From the Eq. (A2.2) through (A2.6), it is easily understood that

$$VB = V\Sigma P^+ = V\Sigma(R^T S_L{}^T + E^T)(S_L RR^T S_L{}^T + EE^T)^{-1} . \tag{B2.3}$$

From the definition of the method, $R = V\Sigma$, where V is an orthonormal basis matrix. Hence

$$VB = RssS_L^T\left(S_L RssS_L^T + \sigma_e^2 I\right)^{-1} . \tag{B2.4}$$

Thus the Imai-Berns model is equivalent to the Wiener Model.

Chapter 3

Noise robustness of a colorimetric evaluation model for image acquisition devices with different characterization models

A colorimetric evaluation of an image acquisition device is important for evaluating and optimizing a set of sensors. Shimano proposed a colorimetric evaluation model [J. Imaging Sci. Technol. 49(6), 588-593 (2005)] based on the Wiener estimation. The mean square errors (MSE) between the estimated and the actual fundamental vectors by the Wiener filter and the proposed colorimetric quality (Qc) agreed quite well with the proposed model and he showed that the estimation of the system noise variance of the image acquisition system is essential for the evaluation model.

In this chapter, it is confirmed that the proposed model can be applied to two different reflectance recovery models and these models provide us an easy method for estimating the proposed colorimetric quality (Qc). The system noise originates from the sampling errors of the spectral characteristics of the sensors, the illuminations and the reflectance and the quantization errors. The influence of the system noise on the evaluation model is studied and it is confirmed from the experimental results that the proposed model holds even in a noisy condition.

3.1 Introduction

Evaluating a color acquisition device is essential for designing optimum sets of sensors. There are two approaches to evaluate a color acquisition device, one is the spectral evaluation and the other is the colorimetric evaluation. These two approaches of the evaluation have each specific purpose.

In the spectral evaluation, the main purpose of the image acquisition device is to obtain the accurate spectral reflectances of objects being imaged in reproducing a color image under a variety of viewing illuminants [1]. The accuracy of the recovered spectral reflectances depends on the number of sensors, their spectral sensitivities, the objects being imaged, the recording illuminants, the noise present in a device and the model used for the recovery. To obtain the spectral reflectances of the imaged objects through the use of sensor responses, several models, such as the Wiener model [2], the multiple regression model [3-10], the Imai-Berns model [11-13] and the Shi-Healey model [14], and the linear model [15-17] have been studied. The optimizations of spectral sensitivities for the acquisition of accurate spectral information of objects are also reported [2,18,19]. Some papers on the optimization of spectral sensitivities for the acquisition of spectral power distributions of illuminants have also been presented [10,12].

On the other hand in colorimetric evaluation, the main purpose of the image acquisition device is to estimate the accurate colorimetric values of the pixels of objects being imaged [20,21]. The accuracy of the estimates depends on the spectral sensitivities of a set of sensors, the objects being imaged, the recording and viewing illuminants, the colorimetric characterization and the noise present in the device. In the past, several models have been proposed to evaluate a colorimetric performance of a set of color sensors. Neugebauer proposed a colorimetric quality factor for the evaluation of a single sensor [22] and Vora and Trussell developed a model to evaluate a set of sensors for the first time [23]. However, the Vora-Trussell model used a random

variable assumption of a surface reflectance. Since a surface spectral reflectance is smooth over the visual wavelengths and falls into a subspace spanned by a small set of basis vectors, their assumption was not adequate. Later, Sharma and Trussell reported a comprehensive analysis to establish the colorimetric quality of an image acquisition device by taking account of the noise effects and statistical properties of spectral reflectance of samples in the tristimulus values, the orthogonal color space and the linearized CIELAB color space [24]. However, the formula by Sharma and Trussell was too complicated to give an intuitive insight into the influence of the noise on color correction and to predict new phenomena. Shimano proposed a simple formula to evaluate colorimetric quality of a set of color sensors by considering the statistical properties of spectral reflectance of samples and noise [25]. By the use of the evaluation models, the optimization of a set of sensors has been performed [26,27]. However, the application of the evaluation models to real color image acquisition devices has not appeared because of the difficulty in estimating noise levels. Recently Shimano proposed a new model to estimate the noise variance of an image acquisition system and applied it to the proposed colorimetric evaluation model [25,28] and spectral evaluation model [29], and confirmed that the both evaluation models agree quite well with the experimental results by multispectral cameras.

For a colorimetric evaluation, color stimuli can be divided into two parts, the fundamental and the residual [30]. The fundamental is a projection of a color stimulus onto the human visual subspace (HVSS) and evokes color sensation to human visual system. The residual is an orthogonal part of the color stimulus and evokes no sensation. In the proposed colorimetric evaluation model, the colorimetric quality Qc is related with the mean square errors (MSE) between the estimated and measured fundamental vectors [31] that are the reflectance vectors projected onto the HVSS. The proposed colorimetric evaluation model is formulated by $\mathrm{MSE}(\sigma^2) = \mathrm{E}_{\max}\left(1 - \mathrm{Q}_c(\sigma^2)\right)$, where $\mathrm{MSE}(\sigma^2)$ is the mean square errors between the recovered

and measured fundamental vectors with the estimated noise variance (σ^2), Emax represents a constant that is determined by the viewing illuminant, the CIE color matching functions and the spectral reflectances of objects and $Qc(\sigma^2)$ is the colorimetric quality of the image acquisition system with the estimated noise variance σ^2. It was shown that $Qc(\sigma^2)$ is determined by the spectral sensitivities of the sensors, the spectral power distribution of the recording and viewing illuminants, the noise variance of the image acquisition device and the spectral reflectances of the imaged objects. The model was applied to the multispectral cameras and it was confirmed that the model agrees quite well with the experimental results, i.e., the $MSE(\sigma^2)$ of the recovered fundamental vectors and the colorimetric quality $Qc(\sigma^2)$ of a set of sensors showed a predicted formulation of $MSE(\sigma^2) = E_{max}\left(1 - Q_c(\sigma^2)\right)$. As $Qc(\sigma^2)$ is derived from Wiener estimation [32], it is very important to confirm whether the model can be applied to other recovery models since the colorimetric quality $Qc(\sigma^2)$ is useful not only for the colorimetric evaluation of an image acquisition device but also for the colorimetric optimization of a set of sensors. In our recent study, we have shown that the quality $Qr(\sigma_r^2)$ of a set of sensors aimed at recovery of spectral reflectances proposed by us can be applied to three different reflectance recovery models [33], where σ_r^2 is the noise variance estimated from the spectral reflectances [34]. But $Qr(\sigma_r^2)$ derived from the reflectance recovery model has little correlation with the colorimetric quality $Qc(\sigma^2)$. For the colorimetric evaluation, it is required to examine that these reflectance recovery models can be applied to the colorimetric quality $Qc(\sigma^2)$ in the human visual subspace spanned by the color matching functions or spectral sensitivities of cones.

In this chapter, it is shown that the relation between $Qc(\sigma^2)$ and $MSE(\sigma^2)$ shows the theoretical prediction of $MSE(\sigma^2)$=Emax(1-$Qc(\sigma^2)$), where the $MSE(\sigma^2)$ is the mean square error of the fundamental vectors recovered by the multiple regression analysis [3-10] and the Imai-Berns model [11-13] by experiments, and the influence of the sampling intervals and the

quantization error of the image data on the evaluation model is examined. From the experimental results, it is confirmed that even in the low signal-to-noise ratio (SNR) conditions, the $\mathrm{Qc}(\sigma^2)$ is also appropriately formulated for these models. Once this linear relation is confirmed, we can estimate $\mathrm{Qc}(\sigma^2)$ by the values of the $\mathrm{MSE}(\sigma^2)$ by the multiple regression model or the Imai-Berns model, without knowing the spectral sensitivities of the sensors, spectral power distribution of recording illuminant or estimating the noise variance and this relation provides us an easier way for the colorimetric evaluation of a real existing image acquisition system.

This chapter is organized as follows. The outline of the colorimetric evaluation model and the models tested are briefly reviewed in section 3.2. In section 3.3, the experimental procedures and the results to demonstrate the trustworthiness of the proposal are described. The final section presents the conclusions.

3.2 Models for the Colorimetric Evaluation

In this section, the derivation of the colorimetric quality $\mathrm{Qc}(\sigma^2)$ to evaluate the color image acquisition system and the models used for the experiments are briefly reviewed.

3.2.1 Wiener Estimation Using Estimated Noise Variance

The visible wavelengths from 400 to 700 nm are sampled at a constant intervals and the number of the samples is denoted as N. A sensor response vector from a set of color sensors for an object with a $\mathrm{N}\times 1$ spectral reflectance vector $\mathbf{r}$ can be expressed by

$$\mathbf{p} = \mathrm{SL}_o\mathbf{r} + \mathbf{e}, \tag{3.1}$$

where $\mathbf{p}$ is a $\mathrm{M}\times 1$ sensor response vector from the M channel sensors, S is a $\mathrm{M}\times\mathrm{N}$ matrix of the spectral sensitivities of sensors in which a row vector represents a spectral sensitivity, L_o is a $\mathrm{N}\times\mathrm{N}$ diagonal matrix with samples of the spectral power distribution of an recording illuminant

along the diagonal, and **e** is a $M \times 1$ additive noise vector. The noise **e** is defined to include all the sensor response errors such as the measurement errors in the spectral characteristics of sensitivities, an illumination and reflectances, and quantization errors in this work and it is termed as the system noise [33] below. The system noise is assumed to be signal independent, zero mean and uncorrelated to itself. For abbreviation, let $S_L = SL_o$. Denote the projection matrix into the HVSS as P_V which is represented by $P_V = \sum_{i=1}^{\alpha} \mathbf{a}_i \mathbf{a}_i^T$, where $\mathbf{a}_i$ is the i-th orthonormal basis vector which spans HVSS and $\alpha = \text{Rank}(TL_V)$. $\{\mathbf{a}_i\}_{i=1,\ldots,\alpha}$ are the right singular vectors determined by the singular value decomposition (SVD) of the matrix TL_V, where T is the $3 \times N$ matrix of CIE color matching functions and L_V is an $N \times N$ diagonal matrix with samples of the spectral power distribution of a viewing illuminant along the diagonal. The projected vector $P_V\mathbf{r}$ is termed a fundamental vector [25,28]. If $\hat{\mathbf{r}}$ represents the recovered spectral reflectance, the mean square errors (MSE) between the actual fundamental vector $P_V\mathbf{r}$ and the recovered fundamental vector $P_V\hat{\mathbf{r}}$ is given by

$$\text{MSE} = E\left\{\left\|P_V\mathbf{r} - P_V\hat{\mathbf{r}}\right\|^2\right\}, \tag{3.2}$$

where $E\{\bullet\}$ represents the expectation. By the Wiener estimation, the matrix W_0 which gives the estimated spectral reflectance $\hat{\mathbf{r}} = W_0\mathbf{p}$ is given by

$$W_0 = \text{Rss}S_L^T\left(S_L\text{Rss}S_L^T + \sigma_e^2 I\right)^{-1}, \tag{3.3}$$

where superscripted T represents the transpose of a matrix, Rss is an autocorrelation matrix of the spectral reflectance of samples that will be captured by a device, and σ_e^2 is the noise variance used for the estimation. Denote the actual system noise variance expressed as σ^2. If σ_e^2 is equal to σ^2, substitution of Eq.(3.3) into Eq.(3.2) leads to [25,28,33]

$$\mathrm{MSE}(\sigma^2) = \sum_{i=1}^{\alpha} \left\| \mathbf{a}_i^{v} \right\|^2 - \sum_{i=1}^{\alpha} \left\| \mathrm{P}_{CV} \mathbf{a}_i^{v} \right\|^2 + \sum_{i=1}^{\alpha} \sum_{j=1}^{\beta} \frac{\sigma^2}{\kappa_j^{v\,2} + \sigma^2} \left(\mathbf{b}_j^{v\,T} \mathbf{a}_i^{v} \right)^2, \tag{3.4}$$

where $\mathbf{b}_i^{v}$, κ_j^{v} and β represent the i-th right singular vector, j-th singular value and a rank of a matrix $S_L V \Lambda^{1/2}$, respectively. The column vector $\mathbf{a}_i^{v}$ is given by $\mathbf{a}_i^{v} = \Lambda^{1/2} V^T \mathbf{a}_i$, Rss is represented as $\mathrm{Rss} = V \Lambda V^T$, where V is a basis matrix and Λ is a $N \times N$ diagonal matrix with positive eigenvalues λ_i along the diagonal in decreasing order, P_{CV} is the projection matrix onto the subspace spanned by a set of basis vectors $\left\{ \mathbf{b}_i^{v} \right\}_{i=1,\ldots,\beta}$ and represented by $\mathrm{P}_{CV} = \sum_{i=1}^{\alpha} \mathbf{b}_i^{v} \mathbf{b}_i^{v\,T}$.

The first and second terms on the right-hand side of the Eq.(3.4) represent the MSE for the noiseless case, which is denoted as $\mathrm{MSE}_{\mathrm{free}}$

$$\mathrm{MSE}_{\mathrm{free}} = \sum_{i=1}^{\alpha} \left\| \mathbf{a}_i^{v} \right\|^2 - \sum_{i=1}^{\alpha} \left\| \mathrm{P}_{CV} \mathbf{a}_i^{v} \right\|^2, \tag{3.5}$$

and the third term corresponds to the increase in the MSE due to the presence of the noise, which is denoted as Noise Influence Factor (NIF) below.

$$\mathrm{NIF} = \sum_{i=1}^{\alpha} \sum_{j=1}^{\beta} \frac{\sigma^2}{\kappa_j^{v\,2} + \sigma^2} \left(\mathbf{b}_j^{v\,T} \mathbf{a}_i^{v} \right)^2. \tag{3.6}$$

Therefore the colorimetric quality of a set of color sensors in the presence of noise is formulated as

$$\mathrm{Q}_c(\sigma^2) = \frac{\sum_{i=1}^{\alpha} \left\| \mathrm{P}_{CV} \mathbf{a}_i^{v} \right\|^2 - \sum_{i=1}^{\alpha} \sum_{j=1}^{\beta} \frac{\sigma^2}{\kappa_j^{v\,2} + \sigma^2} \left(\mathbf{b}_j^{v\,T} \mathbf{a}_i^{v} \right)^2}{\sum_{i=1}^{\alpha} \left\| \mathbf{a}_i^{v} \right\|^2}. \tag{3.7}$$

Hence, the $\mathrm{MSE}(\sigma^2)$ is expressed as

$$\mathrm{MSE}(\sigma^2) = \mathrm{E}_{\max}\left(1 - \mathrm{Q}_c(\sigma^2)\right), \tag{3.8}$$

where $\mathrm{E}_{\max} = \sum_{i=1}^{\alpha} \left\| \mathbf{a}_i^v \right\|^2$. This equation shows that the $\mathrm{MSE}(\sigma^2)$ has a linear relation to $\mathrm{Qc}(\sigma^2)$ and the slope of the line is $\sum_{i=1}^{\alpha} \left\| \mathbf{a}_i^v \right\|^2$. The values of $\sum_{i=1}^{\alpha} \left\| \mathbf{a}_i^v \right\|^2$ are dependent only on the viewing illuminant, the CIE color matching functions and the surface spectral reflectance of the objects being captured. The $\mathrm{MSE}(\sigma^2)$ decreases as the $\mathrm{Qc}(\sigma^2)$ increases to one.

The first term on the right-hand side of the Eq.(3.4), $\sum_{i=1}^{\alpha} \left\| \mathbf{a}_i^v \right\|^2$, is considered to represent the Statistical Mean Energy of Color Stimuli (SMECS) which is incident on the cones. The second term on the right-hand side of the Eq.(3.4) represents the energy of the SMECS captured by a set of color sensors. And the third term of it corresponds to the increase in the MSE due to the presence of the noise [25]. Therefore, the colorimetric quality $\mathrm{Qc}(\sigma^2)$ in Eq.(3.7) can be interpreted as the ratio of the energy a set of sensor capture to that of the SMECS.

If we let the noise variance $\sigma_e^2 = 0$ for the Wiener filter in Eq.(3.3), then the $\mathrm{MSE}(0)$ is derived as

$$\mathrm{MSE}(0) = \sum_{i=1}^{\alpha} \left\| \mathbf{a}_i^v \right\|^2 - \sum_{i=1}^{\alpha} \left\| \mathrm{P}_{CV} \mathbf{a}_i^v \right\|^2 + \sum_{i=1}^{\alpha} \sum_{j=1}^{\beta} \frac{\sigma^2}{\kappa_j^{v\,2}} \left(\mathbf{b}_j^{v\,T} \mathbf{a}_i^v \right)^2 , \tag{3.9}$$

where details of the proofs are shown in the previous paper [28].

Then the estimated system noise variance $\hat{\sigma}^2$ can be represented by

$$\hat{\sigma}^2 = \frac{\mathrm{MSE}(0) - \mathrm{MSE}_{\mathrm{free}}}{\sum_{i=1}^{\alpha} \sum_{j=1}^{\beta} \frac{\left(\mathbf{b}_j^{v\,T} \mathbf{a}_i^v \right)^2}{\kappa_j^{v\,2}}} . \tag{3.10}$$

Therefore, the system noise variance σ^2 can be estimated using Eq.(3.10), since the MSEfree and the denominator of Eq.(3.10) can be computed if the surface reflectance spectra of objects,

the spectral sensitivities of sensors and the spectral power distribution of the recording and viewing illuminants are known. The $\mathrm{MSE}(0)$ can also be obtained by the experiment using Eqs. (3.2) and (3.3) applying the Wiener filter with $\sigma_e^2 = 0$ to sensor responses. [25,28]

The colorimetric quality $\mathrm{Qc}(\sigma^2)$ and $\mathrm{MSE}(\sigma^2)$ can be computed by substituting the estimated noise variance to Eq.(3.7) and Eq.(3.2) , respectively.

3.2.2 Application of the Multiple Regression Analysis to Fundamental Vector Evaluation

To achieve the colorimetric evaluation, the multiple regression model is used to recover the fundamental vectors. Let $\mathbf{p}_i$ be a $M \times 1$ sensor response vector which is obtained by the image acquisition of a known spectral reflectance $\mathbf{r}_i$ of the i-th object. Let P be a $M \times k$ matrix which contains the sensor responses $\mathbf{p}_1, \mathbf{p}_2, \cdots, \mathbf{p}_k$, and let F be a $N \times k$ matrix which contains the corresponding fundamental vectors $\mathbf{f}_1, \mathbf{f}_2, \cdots, \mathbf{f}_k$, where $\mathbf{f}_i = P_V \mathbf{r}_i$ and k is the number of the learning samples. The matrix W which minimizes $\|F - WP\|$, where notation $\|\bullet\|$ represents the Frobenius norm[35] is given by.

$$W = FP^+, \tag{3.11}$$

where P^+ represents the pseudo inverse matrix of the matrix P . The estimated fundamental vector $\hat{\mathbf{f}}_i$ is given by $\hat{\mathbf{f}}_i = W\mathbf{p}_i$. Therefore this model does not use the spectral sensitivities of sensors or the spectral power distribution of an illumination, but it uses only the fundamental vectors of the learning samples.

3.2.3 Application of the Imai-Berns Model to Fundamental Vector Evaluation

To achieve the colorimetric evaluation, the Imai-Berns model is applied to estimate the weight matrix in the HVSS and is used to recover the fundamental vectors. The sensor response matrix

P and the fundamental vectors $\mathbf{f}_i$ are defined the same manner as the regression model. Let Σ be a $d \times k$ matrix which contains the column vectors of the weights $\boldsymbol{\sigma}_1, \boldsymbol{\sigma}_2, \cdots, \boldsymbol{\sigma}_k$ to represent the k known fundamental vectors $\mathbf{f}_1, \mathbf{f}_2, \cdots, \mathbf{f}_k$, where d is a number of the weights. The multiple regression analysis between Σ and P is expressed as $\|\Sigma - BP\|$. A matrix B which minimize the Frobenius norm is given by

$$B = \Sigma P^{+} . \tag{3.12}$$

Since a weight column vectors $\boldsymbol{\sigma}_i$ for a sensor response vector $\mathbf{p}_i$ is estimated by $\hat{\boldsymbol{\sigma}}_i = B\mathbf{p}_i$, the estimated fundamental vector is derived from $\hat{\mathbf{f}}_i = V\hat{\boldsymbol{\sigma}}_i$, where a matrix V is the basis matrix which contains first d orthonormal basis of the fundamental vectors. This model does not use the spectral characteristics of sensors or an illumination.

3.3 Experimental Procedures

Detailed experimental procedures and conditions are described in the previous paper [33,34] and the procedures specific to this chapter are described briefly below.

A multispectral color image acquisition system was assembled by using seven interference filters (Asahi Spectral Corporation) in conjunction with a monochrome video camera (Kodak KAI-4021M). The images of a GretagMacbeth ColorChecker (24 colors) and the Kodak Q60R1 (228 Colors), let us denote them CC and KK respectively for abbreviation, were converted to 16-bit-depth digital data by an AD converter. The spectral reflectances of the GretagMacbeth ColorChecker, spectral characteristics of the illumination and the sensors of the camera were measured at 1-nm sampling intervals over wavelength from 400 to 700 nm (Kodak Q60R1 were only measured at 10-nm sampling intervals). Next the least significant bits of the measured 16-bit image data are taken away to simulate various quantization errors and the spectral

characteristics are converted to desired sampling intervals. The measured spectral sensitivities of the camera with each filter are shown in Fig.3.1. The spectral power distribution of the illuminant (Seric Solax XC-100AF) is presented in Fig.3.2.

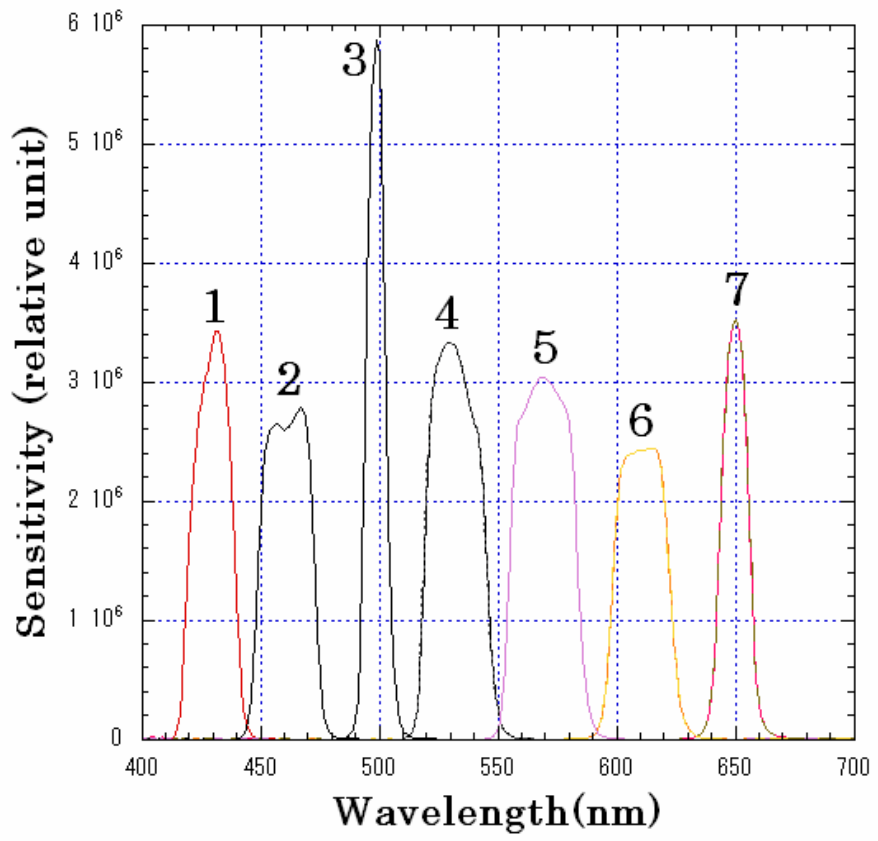

Fig. 3.1. Spectral sensitivities of the sensors of the camera sampled at 1nm.

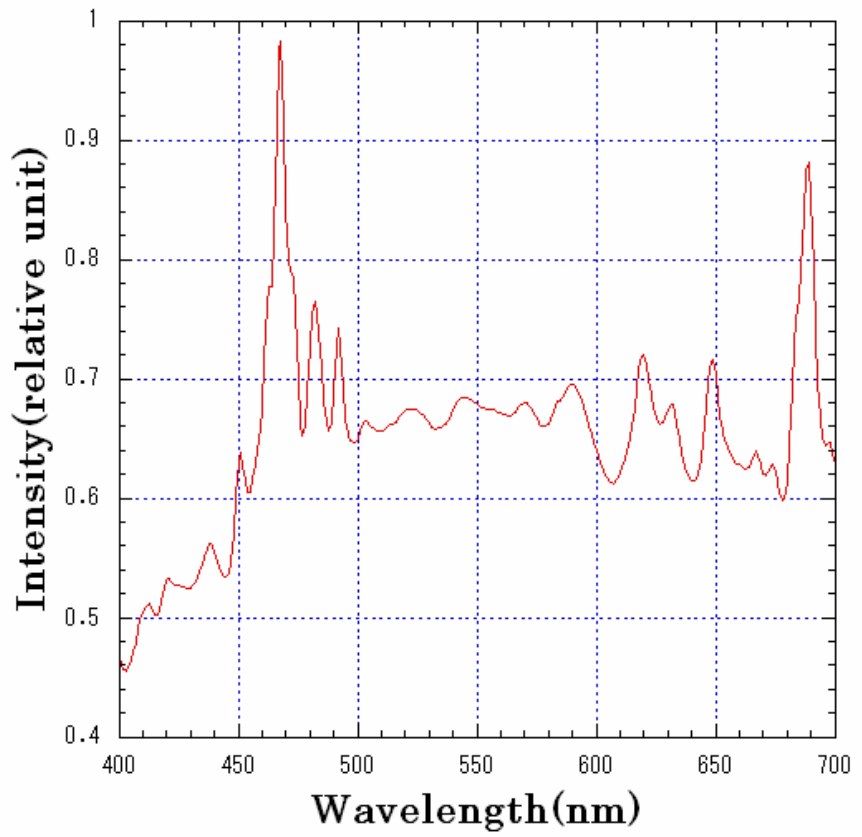

Fig. 3.2. Spectral power distribution of the illumination sampled at 1nm.

By using all combinations of sensors from three to seven sensors sampling at various sampling intervals and the signals with various sampling bit depth, the system noise variance was estimated and the colorimetric quality $Qc(\sigma^2)$ was computed. Then the estimated noise variance was used to recover the fundamental vectors with the spectral reflectance recovered by the Wiener estimation, and then the $MSE(\sigma^2)$ of the recovered fundamental vectors was computed by averaging the difference between actual and recovered fundamental vectors over colors. The fundamental vectors were also recovered by the multiple regression model and the Imai-Berns model and MSE of the recovered fundamental vectors by theses models were computed. By using the estimated noise variance, the colorimetric quality $Qc(\sigma^2)$ for each combination of sensors was computed using Eq.(3.7).

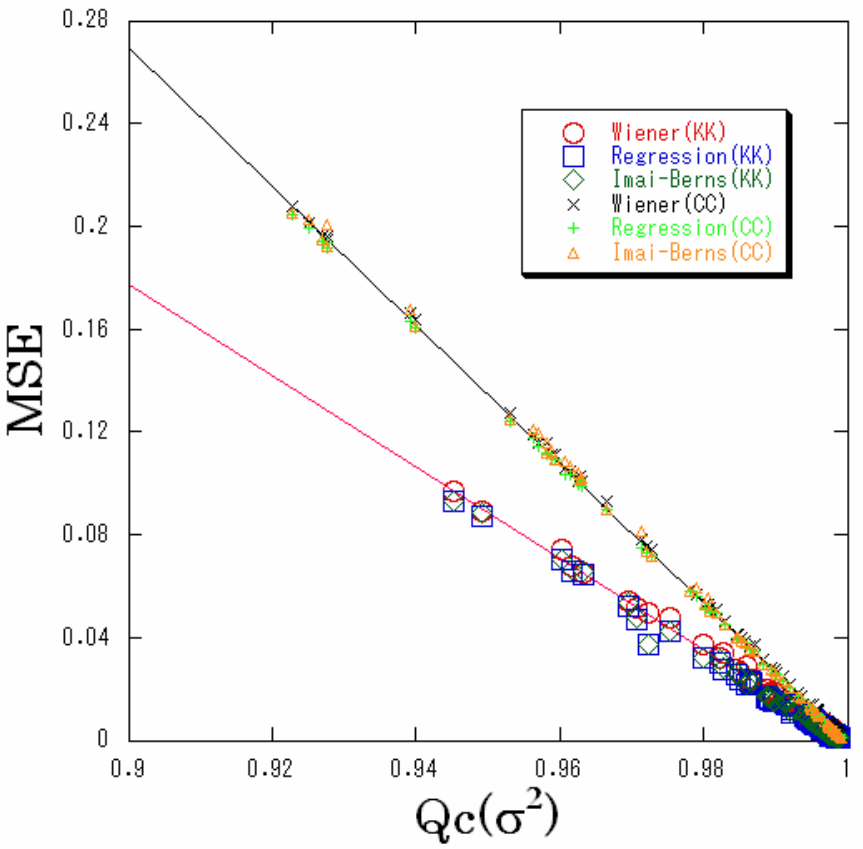

Fig. 3.3. MSEs of the recovered fundamental vectors by the Wiener, Regression, and Imai-Berns model for the GretagMacbeth ColorChecker (CC) and the Kodak Q60R1 (KK) are plotted as a function of $Qc(\sigma^2)$.

3.4 Results and Discussions

In this chapter, the learning sample is the same as the test sample, i.e. , if the test sample is CC then the CC is used as the learning sample.

3.4.1 MSE and Qc (σ^2)

The plots of the $MSE(\sigma^2)$ of the CC and KK as a function of $Qc(\sigma^2)$ with 16-bit image and 10-nm sampling intervals for the spectral characteristics of the sensors, the illuminations and the reflectance (16bit-10nm) are shown in Fig.3.3. The lines in the figure show the theoretical

relation between the MSE (σ^2) and Qc (σ^2) as given by Eq.(3.8), where the equation $E_{max} = \sum_{i=1}^{\alpha} \left\| \mathbf{a}_i^v \right\|^2$ determines the slopes of the line for each color chart. The experimental results of the MSE as a function of Qc (σ^2) by the multiple regression analysis and the Imai-Berns model agree well with the theoretical lines. The plots of KK around Qc (σ^2) =0.972 scatter slightly, this might originate from the glossy and undulated surface of the color chart as KK is a printed photograph.

The results in Fig.3.3 agree quite well with the theoretical predictions and show that Qc (σ^2) is able to be used for the multiple regression analysis and the Imai-Berns model. Assuming that the spectral reflectances and the noise have no correlation and that the Imai-Berns model uses all the principal components [36], and approximating the autocorrelation matrix of the noise as $\sigma^2 I$, it is possible to be proved that the multiple regression model and the Imai-Berns model are mathematically equivalent to the Wiener estimation, i.e., the matrixes W given by Eq.(3.11) in the multiple regression model and VB in the Imai-Berns model, where B is given by Eq.(3.12), are equivalent to the matrix $P_V W_0$ in the Wiener estimation [34]. Thus, the MSE (σ^2) of the multiple regression analysis and the Imai-Berns model gives an easy way to estimate the colorimetric quality Qc (σ^2) without complicated computations of Eq.(3.7) or without the information of the spectral characteristics of the imaging system required for the Wiener model.

3.4.2 Effect of the Noise to the Relation between MSE and Qc (σ^2)

Next the influence of the sampling intervals and quantization error on the colorimetric evaluation model is examined. In Fig.3.4(a), the MSE (σ^2) of CC as a function of Qc (σ^2) with 8bit-10nm is shown, and those with 8bit-20nm, 6bit-10nm and 6bit-20nm are shown in Fig.3.4(b), Fig.3.4(c) and Fig.3.4(d), respectively.

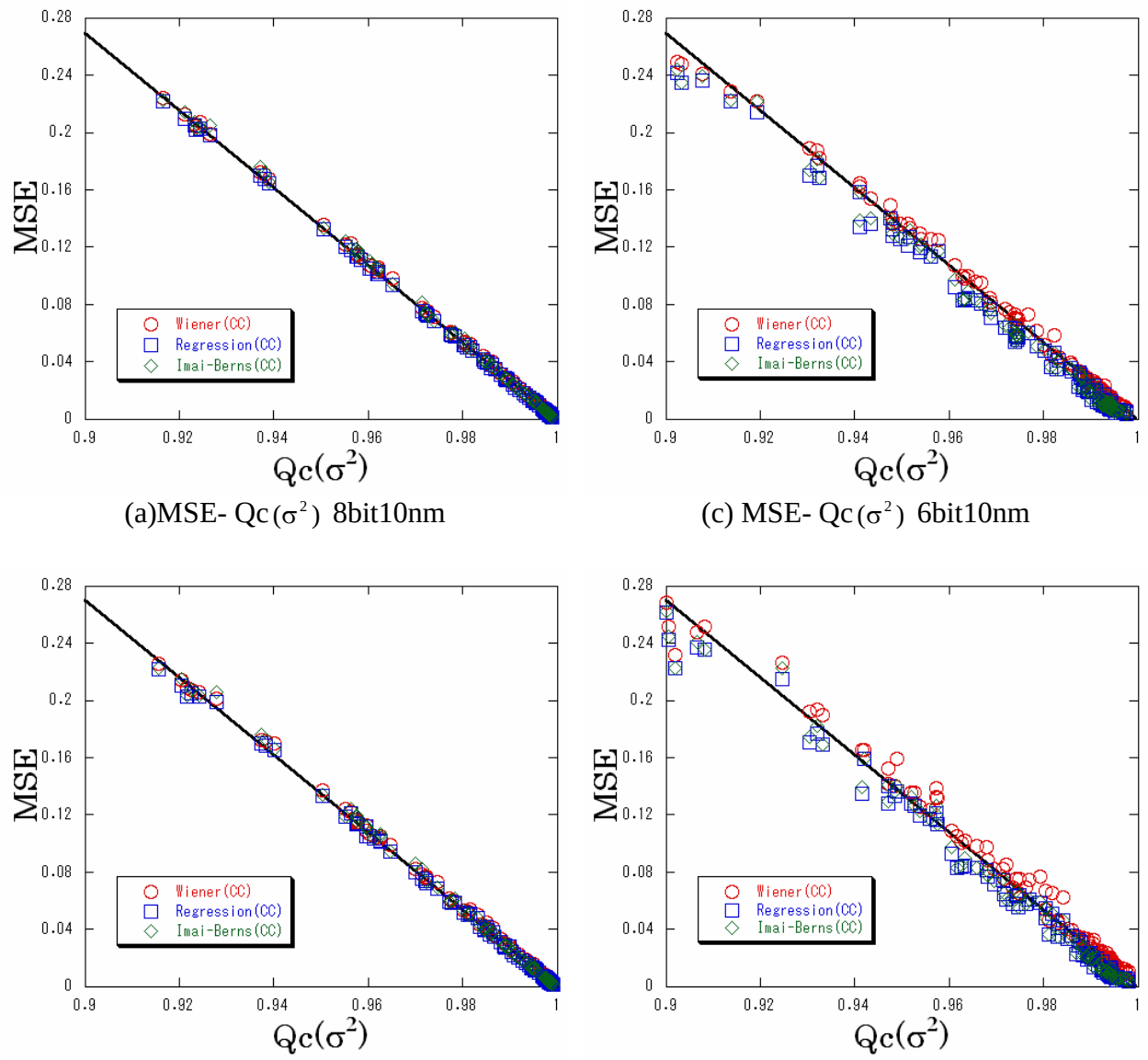

(a)MSE- Qc(σ^2) 8bit10nm

(c) MSE- Qc(σ^2) 6bit10nm

(b) MSE- Qc(σ^2) 8bit20nm

(d) MSE- Qc(σ^2) 6bit20nm

Fig. 3.4. MSEs of the recovered fundamental vectors by the Wiener, Regression, and Imai-Berns model for GretagMacbeth ColorChecker (CC) are plotted as a function of Qc(σ^2) with (a)8-bit image and 10-nm sampling intervals, (b)8-bit image and 20-nm sampling intervals, (c)6-bit image and 10-nm sampling intervals, and (d)6-bit image and 20-nm sampling intervals.

In Fig.3.4(b), although the plots for 8bit-20nm scatter slightly compared to those for 8bit-10nm, the results agree fairly well with the theoretical line. In Fig.3.4(c) and Fig.3.4(d), the plots for 6bit-10nm and 6bit-20nm are still along the theoretical line but they scatter largely compared to those for 8bit-10nm because the system noise variance increases with the larger quantization error or the larger sampling intervals. It is remarkable that the $\mathrm{MSE}(\sigma^2)$ and $\mathrm{Qc}(\sigma^2)$ still show the relation of $\mathrm{MSE}(\sigma^2) = \mathrm{E}_{\max}\left(1 - \mathrm{Q}_c(\sigma^2)\right)$ even with 6bit-20nm.

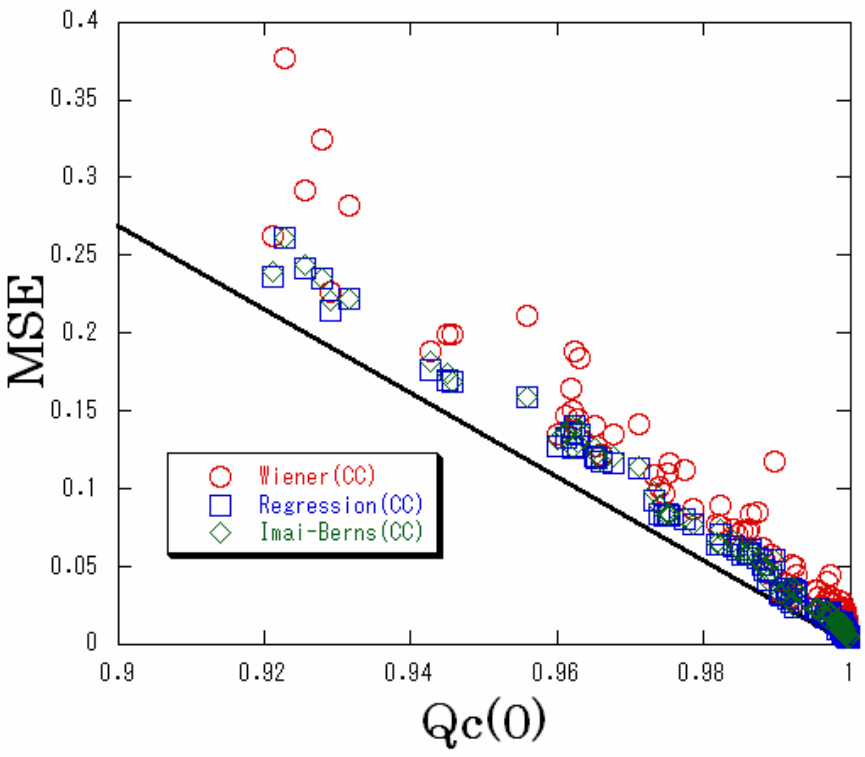

Fig. 3.5. MSEs of the recovered fundamental vectors by the Wiener, Regression, and Imai-Berns model for GretagMacbeth ColorChecker (CC) are plotted as a function of $\mathrm{Qc}(0)$ with 6-bit image and 10-nm sampling intervals ($\mathrm{MSE}(0)$s are plotted for the Wiener model).

To examine the effect of the estimation of the system noise variance, let $Qc(0)$ be the value of $Qc(\sigma^2)$ when the noise variance is not considered, i.e.,

$$Q_c(0) = \frac{\sum_{i=1}^{\alpha} \left\| P_{CV} \mathbf{a}_i^v \right\|^2}{\sum_{i=1}^{\alpha} \left\| \mathbf{a}_i^v \right\|^2} . \tag{3.13}$$

The experimental results on the relation between $Qc(0)$ and $MSE(0)$ correspond to the case where the noise present in the image acquisition device is not taken into account, which are shown with 6bit-10nm in Fig.3.5. The $MSE(0)$ can be obtained by the experiment using Eqs. (3.2) and (3.3) applying the Wiener filter with $\sigma_e^2 = 0$. In Fig.3.5, the plots scatter largely far above the theoretical line. Therefore, this result shows the importance of the estimation of the noise variance in the evaluation model.

3.4.3 Effect of the Sampling Bits to MSE

Since the plots with 6bit-10nm scatters more than those with 8bit-20nm, to examine the effect of the quantization error to the evaluation model, the most and least quantization error sensitive sensor sets with 10-nm sampling interval are selected by the increase in the absolute error to the theoretical MSE which is calculated by the Eq.(3.8) for 8-bit and 6-bit image. The sensor set "247" has the least increase in the absolute error and the sensor set "1234" has the most increase in the absolute error when quantization error is increased by changing the image data from 8-bit to 6-bit. It is interesting to see that the least quantization error sensitive sensor set "247" has little decrease in the colorimetric quality $Qc(\sigma^2)$, which is 0.988979 for 8-bit image and 0.987561 for 6-bit image, and the most quantization error sensitive sensor set "1234" has a large decrease in the colorimetric quality $Qc(\sigma^2)$,which is 0.923537 for 8-bit image and 0.903407 for 6-bit image.

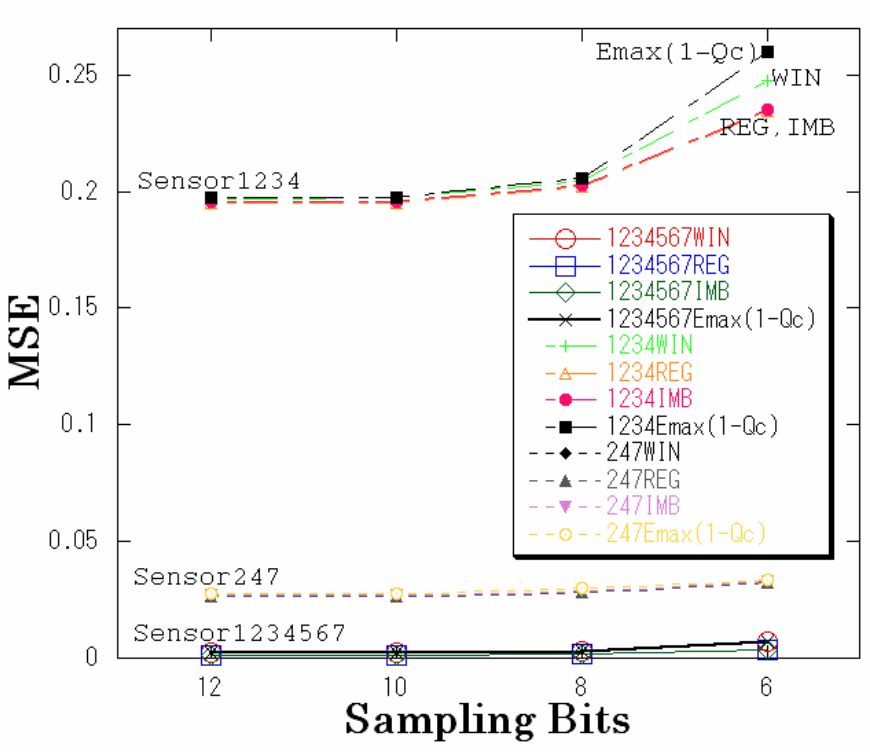

Fig. 3.6. MSEs of the recovered fundamental vectors by the Wiener, Regression, and Imai-Berns model for GretagMacbeth ColorChecker (CC) and the theoretical MSE estimated with Emax(1-$Qc(\sigma^2)$) with 10-nm sampling intervals are plotted as a function of the sampling bits.

In Fig.3.6, the MSE as a function of the sampling bits by the three recovery models are shown. For the sensor set “247” or “1234567”, though the MSE increases as the sampling bit decreases, the MSE of the three model show very close value to the theoretical MSE estimated from the $Qc(\sigma^2)$ with the Eq.(3.8). On the other hand, the MSE of the sensor set “1234” of the 6-bit sampling is different from the value of the theoretical MSE. This means that the estimation of the MSE by the colorimetric quality $Qc(\sigma^2)$ is not accurate for a set of sensors which are sensitive to the quantization error at the 6-bit sampling images.

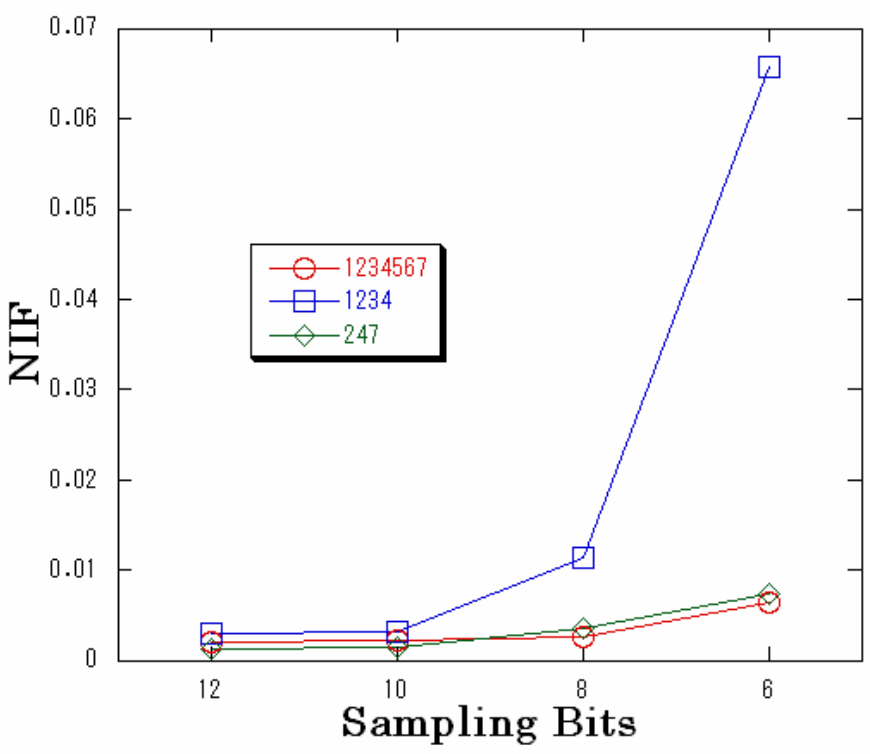

Fig. 3.7. 10nm NIF(Noise Influence Factor) for three sensor sets are plotted as a function of the sampling bits.

3.4.4 Effect of the Sampling Bits to NIF

The Eq.(3.4) can be written as

$$\mathrm{MSE}(\sigma^2) = \mathrm{MSE}_{\mathrm{free}} + \mathrm{NIF}, \tag{3.14}$$

where MSEfree represents the MSE for the noiseless case and NIF represents the increase in the MSE due to the presence of the noise. Since the MSEfree is free from the sampling bits of the image data, the increase in the MSE with the sampling bits originates from the increase in the NIF. To examine the effect of the sampling bits to the Eq.(3.14), the relation between the sampling bits and NIF is shown in Fig.3.7. It is clear that the sensor set “1234” is sensitive to the

quantization error compared to the other sensor sets, “1234567” or “247” because the NIF for the sensor set “1234” increases as the sampling bit decreases.

3.4.5 Reason of the Noise Sensitivity

The estimated noise variance and the squared singular values as a function of the dimensions for each sensor set “1234” and “247” sampling at 10-nm intervals are shown in Fig.3.8. From the Eq.(3.6), it is easily seen that NIF shows a small value when the squared singular value is larger than the noise variance. In Fig.3.8, the squared singular values of the sensor set “247” decrease as the dimension increase but the third (the smallest) squared singular value ($\kappa_3^{v^2}$) is still far larger than the noise variance of “247-6bit”. On the other hand for the sensor set “1234”, the squared singular values decrease rapidly compared to those of the sensor set “247”. And the third squared singular value ($\kappa_3^{v^2}$) is almost the same as the noise variance of “1234-6bit”, the fourth (the smallest) squared singular value ($\kappa_4^{v^2}$) is smaller than the noise variance of “1234-6bit” and almost reaching to the noise variance of “1234-8bit”. These two small singular values make the sensor set “1234” vulnerable to the noise.

Thus the first reason for the noise sensitivity of the sensor set “1234” is the rapid decreasing singular values. The second reason is the large noise variance of the sensor set “1234” itself, which is several times larger than that of other sensor sets. The approximation for the autocorrelation matrix of the noise as $\sigma^2 I$ in this proposal makes the MSE by the Wiener model slightly different from those of the regression model or the Imai-Berns model.

3.4.6 Error and Quality Estimation Model

From the experiments, it is confirmed that the colorimetric quality $Qc(\sigma^2)$ can be applied to the regression model and the Imai-Berns model, and that $Qc(\sigma^2)$ can be estimated by the multiple regression model or the Imai-Berns model without prior knowledge of the spectral

sensitivities of the set of sensors, spectral power distribution of an illumination and the noise present in the image acquisition system, since the point (which represents the MSE determined by the experiments) on the theoretical line gives us the estimate of the colorimetric quality $Qc(\sigma^2)$. Therefore, the quality can be easily estimated without the difficult computations. The experiments also showed that the colorimetric quality $Qc(\sigma^2)$ is robust to the increase in the system noise with the low-SNR images .

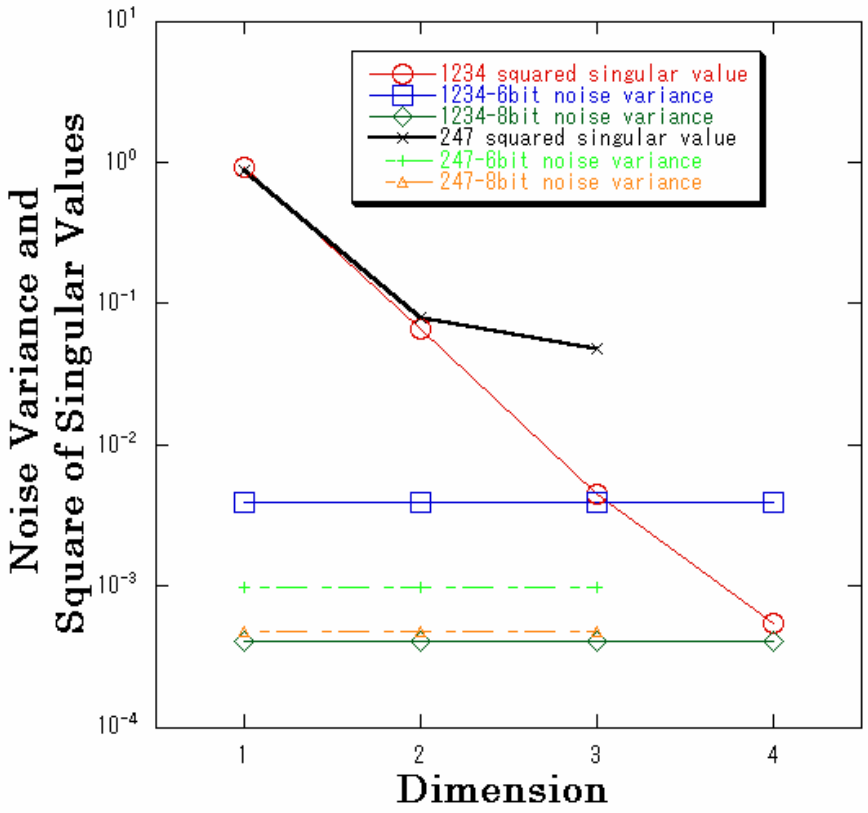

Fig. 3.8. Noise variance and the square of singular values for the sensor set “1234” and “247” with 8-bit and 6-bit images, 10-nm sampling intervals.

3.5 Conclusions

The colorimetric evaluation model derived from the Wiener estimation was applied to the multiple regression analysis and the Imai-Berns method, and the influence of the quantization errors and sampling intervals of an image acquisition system on the evaluation was studied. The experimental results agree quite well with the predictions by the model even in a noisy condition.

Experimental results show that the colorimetric evaluation model is robust to the increase in the system noise with the sampling errors or the quantization errors.

It is concluded that the proposed colorimetric evaluation model is appropriately formulated and effective even in a noisy condition and that the estimation of the system noise variance of an image acquisition system is essential to evaluate the colorimetric quality $Qc(\sigma^2)$ [37,38].

The relation of $MSE(\sigma^2) = E_{max}\left(1 - Q_c(\sigma^2)\right)$ gives us an easy method to estimate the colorimetric quality $Qc(\sigma^2)$ by the $MSE(\sigma^2)$ and this result provides us an easier way for the determination of the colorimetric quality of an image acquisition system without the spectral characteristics of the sensors, the recording illuminant or the noise present in the image acquisition system.

References

1. Y. Miyake and Y. Yokoyama, "Obtaining and Reproduction of Accurate Color Images Based on Human Perception", Proc. SPIE **3300**, 190-197(1998).
2. H. Haneishi, T. Hasegawa, N. A. Hosoi, Y. Yokoyama, N. Tsumura and Y. Miyake, "System design for accurately estimating the spectral reflectance of art paintings", Appl. Optics, **39**,6621-6632(2000).
3. Y. Zhao, L.A. Taplin, M. Nezamabadi and R.S. Berns, “Using the Matrix R Method for Spectral Image Archives”, The 10th Congress of the International Color Association (AIC’5), (Granada, Spain), pp.469-472 (2005).
4. K. Martinez, J. Cupitt, D. Saunders and R. Pillay, "Ten Years of Art Imaging Research", Proc. of the IEEE, **90**,28-41(2002).
5. A. A. Afifi and S. P. Azen, "Statistical Analysis", Chap.3,(Academic Press,1972).
6. H. L. Shen and J. H. Xin, "Spectral characterization of a color scanner based on optimized adaptive estimation", J. Opt. Soc. Am. A**23**, 1566-1569(2006).
7. D. Connah, J. Y. Hardeberg, and S. Westland, "Comparison of Linear Spectral Reconstruction Methods for Multispectral Imaging", Proc. IEEE's International Conference on image Processing (IEEE,2004),pp.1497-1500.
8. Y. Zhao, L. A. Taplin, M. Nezamabadi, and R. S. Berns, "Methods of Spectral Reflectance Reconstruction for A Sinarback 54 Digital Camera", Munsell Color Science Laboratory Technical Report December 2004,pp.1-36(2004).
9. D. Connah and J. Y. Hardeberg, "Spectral recovery using polynomial models” Proc. SPIE **5667**, 65-75 (2005)
10. M. A. López-Álvarez, J. Hernández-Andrés, J. Romero, F. J. Olmo, A. Cazorla, and L. Alados-Arboledas, "Using a trichromatic CCD camera for spectral skylight estimation," Appl. Opt. **47**, H31-H38 (2008).
11. F.H. Imai and R.S. Berns, "Spectral Estimation Using Trichromatic Digital Cameras", Proc. Int. Symposium on Multispectral Imaging and Color Reproduction for Digital Archives, Chiba, Japan. 42-49, (1999).

12. M. A. López-Álvarez, J. Hernández-Andrés, Eva. M. Valero and J. Romero, "Selecting algorithms, sensors and liner bases for optimum spectral recovery of skylight" J. Opt. Soc. Am. A**24**,942-956(2007).
13. V. Cheung, S. Westland, C. Li, J. Hardeberg and D. Connah, "Characterization of trichromatic color cameras by using a new multispectral imaging technique", J. Opt. Soc. Am. A**22**, 1231-1240(2005).
14. M. Shi and G. Healey, “Using reflectance models for color scanner calibration”, J. Opt. Soc. Am. A **19**(4), 645-656 (2002).
15. J. Cohen, "Dependency of spectral reflectance curves of the Munsell color chips," Psychon. Sci. **1**, 369-370 (1964).
16. L. T. Maloney, "Evaluation of linear models of surface spectral reflectance with small numbers of parameters," J. Opt. Soc. Am. A **3**, 1673-1683 (1986).
17. J. P. S. Parkkinen, J. Hallikainen, and T. Jaaskelainen,"Characteristic spectra of Munsell colors," J. Opt. Soc. Am. A **6**, 318-322 (1989).
18. R. Piché, "Nonnegative color spectrum analysis filters from principal component analysis characteristic spectra," J. Opt. Soc. Am. A **19**, 1946-1950 (2002)
19. M. Mahy, P. Wambacq, L. Van Eycken, and A. Oosterlinck, "Optimal filters for the reconstruction and discrimination of reflectance curves," Proc. IS&T/SID's 2nd Color Imaging Conf., pp. 140–143 (1994).
20. P.S. Hung, “Colorimetric calibration for scanners and media,” Proc. SPIE **1448**, 164-174 (1991).
21. H.R. Kang, “Colorimetric scanner calibration”, J. Imaging Sci. Technol. **36**(2), 162-170 (1992).
22. H.E.J. Neugebauer “Quality factor for filters whose spectral transmittances are different from color mixture curves, and its application to color photography.” J. Opt. Soc. Am. **46**(10),821-824 (1956)
23. P.L. Vora and H.J. Trussell, “Measure of goodness of a set of color-scanning filters,” J. Opt. Soc. Am. A **10**(7), 1499-1508 (1993).

24. G. Sharma and H.J. Trussell, “Figure of merit for color scanners,” IEEE Trans. Image Process. **6**(7), 990-1001 (1997).
25. N. Shimano, “Suppression of noise effect in color corrections by spectral sensitivities of image sensors,” Opt. Rev. **9**(2), 81-88 (2002).
26. N. Shimano, "Optimization of spectral sensitivities with Gaussian distribution functions for a color image acquisition device in the presence of noise", Optical Engineering, vol.**45**(1)., pp.013201-1-8, (2006).
27. G. Sharma, H.J. Trussell and M.J. Vrhel, “Optimal nonnegative color scanning filters,” IEEE Trans Image Process. **7**(1), 129-133 (1998).
28. N. Shimano, “Application of a Colorimetric Evaluation Model to Multispectral Color Image Acquisition Systems” J. Imaging Sci. Technol. **49**(6), 588-593 (2005).
29. N. Shimano, "Evaluation of a multispectral image acquisition system aimed at reconstruction of spectral reflectances", Optical Engineering, vol.**44**, pp.107115-1-6, (2005).
30. J. B. Cohen, "Color and color mixture: Scalar and vector fundamentals," Color Res. Appl., vol. **13**, (1), pp. 5-39, (1988).
31. W. A. Shapiro, "Generalization of Tristimulus Coordinates," J. Opt. Soc. Am. **56**, 795 (1966)
32. A. Rosenfeld and A. C. Kak, Digital Picture Processing, 2nd ed., (Academic Press, 1982).
33. N. Shimano, "Recovery of Spectral Reflectances of Objects Being Imaged Without Prior Knowledge" IEEE Trans. Image Process. vol. **15**, no.7, pp. 1848-1856, Jul. (2006).
34. M. Hironaga and N. Shimano, “Evaluating the Quality of an Image Acquisition Device Aimed at the Reconstruction of Spectral Reflectances Using Recovery Models”, J. Imaging Sci. Technol. 52, 030503 (2008).
35. G.H. Golub and C.F.V. Loan, "Matrix Computations", 3rd ed. (The Johns Hopkins Univ. Press, 1996), p.55.
36. M. A. López-Álvarez, J. Hernández-Andrés and J. Romero, "Developing an optimum computer-designed multispectral system comprising a monochrome CCD camera and a liquid-crystal tunable filter," Appl. Opt. **47**, 4381-4390 (2008).
37. M. Hironaga, N. Shimano, "Noise robustness of a colorimetric evaluation model for image acquisition devices with different characterization models," Appl. Opt. 48, 5354-5362 (2009).

38. M. Hironaga, N. Shimano, "Colorimetric Evaluation of a Set of Spectral Sensitivities", CGIV 2008, 4th European Conference on Colour in Graphics, Imaging, and MCS/08 602-607, Terrassa, Spain (2008).

Chapter 4

Influence of the noise present in an image acquisition system on the accuracy of recovered spectral reflectances

A noise plays an important role in the image acquisition to solve an inverse problem such as the reconstruction of spectral reflectances of the imaged objects by use of the sensor responses. Usually a recovered spectral reflectance $\hat{\mathbf{r}}$ by a matrix W is expressed by $\hat{\mathbf{r}}$ =W**p**, where **p** is a sensor response.

In this chapter, the mean square errors (MSE) between the recovered spectral reflectances with various reconstruction matrices W and actual spectral reflectances are divided into the noise independent MSE (MSE_{FREE}) and the noise dependent MSE (MSE_{NOISE}). By dividing the MSE into two terms, the MSE_{NOISE} is defined as the estimated noise variance multiplied by the sum of the squared singular values of the matrix W. It is shown that the relation between the increase in the MSE and the MSE_{NOISE} agrees quite well in the experimental results by the multispectral camera and that the estimated noise variances are in the same order of the magnitude for various matrices W but the increase in the MSE by the noise mainly results from the increase in the sum of the squared singular values for the unregularized reconstruction matrix W.

4.1 Introduction

The reconstruction of accurate spectral reflectances of an object by the use of an image acquisition device is very important to reproduce color images under a variety of viewing illuminants or to establish color constancy. The recovery performance depends on the number of the sensors, their spectral sensitivities, the objects being imaged, the recording illuminants, the noise present in a device and the model used for the recovery. Therefore the evaluation of the image acquisition devices is important for the optimization of the devices and for the acquisition of the accurate spectral information. Several models have been proposed to evaluate a colorimetric performance of a set of color sensors [1-4], and the optimization of a set of sensors has been carried out on the evaluation models [5,6]. The estimation of the noise present in the image acquisition system is required for the accurate evaluation of the image acquisition device. Shimano proposed a model to estimate the noise variance of an image acquisition system [7] and applied it to the proposed colorimetric evaluation model and a spectral evaluation model, and confirmed that the evaluation model agrees quite well with the experimental results by multispectral cameras [8-12]. He also proposed the Noise Influence Factor to evaluate the influence of the noise on the accuracy of the estimated colorimetric values [13] and on the recovered spectral reflectances [14].

In this chapter, the influence of the reconstruction models on the recovery performances in the presence of the noise is addressed. We propose a model to separate the MSE (mean square errors) of the recovered reflectances into the noise independent MSE_{free} and the noise dependent MSE_{noise}. For the first time, a method to estimate the noise variance of an image acquisition device is derived for various reconstruction matrices W by separating the MSE into two terms. The experimental results show that the increase in the MSE by the noise agrees quite well with

the proposed model. From the experimental results, it is shown that the estimated noise variances are almost independent to the reconstruction matrix W but the sum of the squared singular values is largely dependent on the reconstruction matrix W.

This chapter is organized as follows. The outline of the model and the method to estimate the noise variance and the models tested are briefly reviewed in the sections 4.2 and 4.3. In the following sections 4.4 and 4.5, the experimental procedures and the results to demonstrate the trustworthiness of the proposal are described. The final section 4.6 presents conclusions

4.2. Models

In this section, the previous models to estimate the noise variance and the models used for the experiments are briefly reviewed.

4.2.1 Previous Models to Separate the MSE based on the Wiener Estimation [7]

A vector space notation for color reproduction is useful in the problems. In this approach, the visible wavelengths from 400 to 700 nm are sampled at constant intervals and the number of the samples is denoted as N. A sensor response vector from a set of color sensors for an object with an $N \times 1$ spectral reflectance vector $\mathbf{r}$ can be expressed by

$$\mathbf{p} = SL\mathbf{r} + \mathbf{e}, \tag{4.1}$$

where $\mathbf{p}$ is an $M \times 1$ sensor response vector from the M channel sensors, S is an $M \times N$ matrix of the spectral sensitivities of sensors in which a row vector represents a spectral sensitivity, L is an $N \times N$ diagonal matrix with samples of the spectral power distribution of an illuminant along the diagonal, and $\mathbf{e}$ is an $M \times 1$ additive noise vector. The noise $\mathbf{e}$ is defined to include all the sensor response errors such as the measurement errors in the spectral characteristics of sensitivities, an illumination and reflectances, and quantization errors resulting from the analog-

to-digital (AD) conversions in this work and it is termed as the system noise [7] below. The system noise is assumed to be signal independent, zero mean and uncorrelated to itself. For abbreviation, let $S_L = SL$. The MSE of the recovered spectral reflectances $\hat{\mathbf{r}}$ is given by

$$\text{MSE} = E\left\{\left\|\mathbf{r} - \hat{\mathbf{r}}\right\|^2\right\}, \tag{4.2}$$

where $E\{\bullet\}$ represents the expectation. If $\hat{\mathbf{r}}$ is given by $\hat{\mathbf{r}} = W\left(\sigma_e^2\right)\mathbf{p}$, then the Wiener matrix $W\left(\sigma_e^2\right)$ is given by

$$W\left(\sigma_e^2\right) = RssS_L^T\left(S_L R_{SS} S_L^T + \sigma_e^2 I\right)^{-1}, \tag{4.3}$$

where T represents the transpose of a matrix, Rss is the autocorrelation matrix of the spectral reflectances of the samples, and σ_e^2 is the noise variance used for the estimation. Substitution of Eq.(4.3) into Eq.(4.2) and by letting $\sigma_e^2 = \sigma^2$ leads to [7]

$$\text{MSE}(\sigma^2) = \sum_{i=1}^{N}\lambda_i - \sum_{i=1}^{N}\sum_{j=1}^{R}\lambda_i b_{ij}^2 + \sum_{i=1}^{N}\sum_{j=1}^{R}\frac{\sigma^2}{\kappa_j^{v\,2} + \sigma^2}\lambda_i b_{ij}^2, \tag{4.4}$$

where λ_i is the eigenvalues of the Rss, b_{ij}, κ_j^v and R represent the i-th row of the j-th right singular vector, the singular value and the rank of the matrix $S_L V\Lambda^{1/2}$, respectively, σ^2 is the actual system noise variance, V is a basis matrix and Λ is an $N \times N$ diagonal matrix with positive eigenvalues λ_i along the diagonal in decreasing order. The first and second terms of the Eq.(4.4) represent the MSE_{free} (the noise independent MSE) and the third term represents the $\text{MSE}_{\text{noise}}$ (the noise dependent MSE) which was previously termed Noise Influence Factor for reflectances (NIFr).

The system noise variance $\hat{\sigma}^2$ can be estimated by [7]

$$\hat{\sigma}^2 = \frac{\mathrm{MSE}(0) - \mathrm{MSE}_{\mathrm{free}}}{\sum_{i=1}^{N}\sum_{j=1}^{R} \frac{\lambda_i b_{ij}^2}{\kappa_j^{v\,2}}}, \tag{4.5}$$

where MSE(0) represents the MSE when $\sigma_e^2 = 0$ is used for the Wiener estimation.

4.2.2 Multiple Regression Analysis [15]

Let $\mathbf{p}_i$ be an $M \times 1$ sensor response vector that is obtained by the image acquisition of a known spectral reflectance $\mathbf{r}_i$ of the i-th object. Let P be an $M \times k$ matrix that contains the sensor responses $\mathbf{p}_1, \mathbf{p}_2, \cdots, \mathbf{p}_k$, and let R be an $N \times k$ matrix that contains the corresponding spectral reflectances $\mathbf{r}_1, \mathbf{r}_2, \cdots, \mathbf{r}_k$, where k is the number of the learning samples. The regression model is to find a matrix W_R which minimizes $\|R - W_R P\|$, where notation $\|\bullet\|$ represents the Frobenius norm [16]. The matrix W_R is given by.

$$W_R = RP^+, \tag{4.6}$$

where, P^+ represents the pseudoinverse matrix of the matrix P. By applying a matrix W_R to a sensor response vector $\mathbf{p}$, i.e., $\hat{\mathbf{r}} = W_R \mathbf{p}$, a spectral reflectance is estimated. This model does not use the spectral sensitivities of sensors or the spectral power distribution of an illumination, but it uses only the spectral reflectances of the learning samples.

4.2.3 Imai-Berns Model[17]

The Imai-Berns model is considered as the modification of the linear model by using the multiple regression analysis between the weight column vectors for basis vectors to represent the known spectral reflectances and corresponding sensor response vectors.

Let Σ be a $d \times k$ matrix that contains the column vectors of the weights $\boldsymbol{\sigma}_1, \boldsymbol{\sigma}_2, \cdots, \boldsymbol{\sigma}_k$ to represent the k known spectral reflectances $\mathbf{r}_1, \mathbf{r}_2, \cdots, \mathbf{r}_k$ and let P be an $M \times k$ matrix that

contains corresponding sensor response vectors of those reflectances $\mathbf{p}_1, \mathbf{p}_2, \cdots, \mathbf{p}_k$,where d is a number of the weights to represent the spectral reflectances. The multiple regression analysis between these matrices is expressed as $\|\Sigma - BP\|$. A matrix B that minimizes the Frobenius norm is given by

$$B = \Sigma P^{+}. \tag{4.7}$$

Since a weight column vectors $\boldsymbol{\sigma}$ for a sensor response vector $\mathbf{p}$ is estimated by $\hat{\boldsymbol{\sigma}} = B\mathbf{p}$, the estimated spectral reflectance vector is recovered by $\hat{\mathbf{r}} = \mathbf{V}\hat{\boldsymbol{\sigma}}$, where a matrix V is the basis matrix that contains first d orthonormal basis vectors of spectral reflectances. This model does not use the spectral characteristics of sensors or an illumination.

Thus the reconstruction matrix W_I , that gives $\hat{\mathbf{r}} = W_I\mathbf{p}$ for the Imai-Berns model is given by

$$W_I = VB. \tag{4.8}$$

4.2.4 Linear Model [18,19]

Assuming the spectral reflectances $\mathbf{r}_1, \mathbf{r}_2, \cdots, \mathbf{r}_k$, are smooth over the visible wave length, the spectral reflectances can be written by

$$\mathbf{r} = V\boldsymbol{\sigma} \tag{4.9}$$

with the basis matrix V and the column vectors of the weights $\boldsymbol{\sigma}$. By letting the system noise $\mathbf{e}$ in Eq.(4.1) equals 0, the sensor response can be written as

$$\mathbf{p} = S_L\hat{\mathbf{r}}. \tag{4.10}$$

Thus the reconstruction matrix W_L , which gives $\hat{\mathbf{r}} = W_L\mathbf{p}$ for the linear model is given by

$$W_L = V(S_L V)^+ . \tag{4.11}$$

4.3 Proposed Model

The previous model was derived from the Wiener matrix. The new proposal is an extension of the previous model, which gives a framework to analyze the influence of the noise or to estimate the noise variance in the system not only for the Wiener matrix but also for other reconstruction matrices.

Let W be a reconstruction matrix, then $\hat{\mathbf{r}} = W(S_L \mathbf{r} + \mathbf{e})$ and the MSE is given by

$$MSE = Tr\left[E\left\{(\mathbf{r} - \hat{\mathbf{r}}) \cdot (\mathbf{r} - \hat{\mathbf{r}})^T\right\}\right], \tag{4.12}$$

$$= Tr\left[E\left\{((I_N - WS_L)\mathbf{r} - W\mathbf{e}) \cdot \left(\mathbf{r}^T (I_N - WS_L)^T - \mathbf{e}^T W^T\right)\right\}\right], \tag{4.13}$$

where I_N is an $N \times N$ identity matrix. We assume that the reflectance $\mathbf{r}$ and the error $\mathbf{e}$ has no correlation, thus $E\{\mathbf{r}\mathbf{e}^T\} = 0$ and $E\{\mathbf{e}\mathbf{r}^T\} = 0$, and let $E(\mathbf{e}\mathbf{e}^T) = \sigma^2 I_M$, where I_M is an $M \times M$ identity matrix, the MSE is given as

$$MSE = Tr\left\{(I_N - WS_L) E\{\mathbf{r}\mathbf{r}^T\} (I_N - WS_L)^T\right\} + \sigma^2 \sum_{i=1}^{R} \kappa_i^{\,2}, \tag{4.14}$$

where the singular value decomposition (SVD) as $W = \sum_{i=1}^{R} \kappa_i \mathbf{w}_i \mathbf{u}_i^{\,t}$ is used. κ_i, $\mathbf{w}_i$ and $\mathbf{u}_i$ are the i-th singular value, the i-th left and right singular vector of the matrix W, respectively.

We denote the first term of the Eq.(4.14) as MSE_{FREE} (the noise independent MSE) and the second term as MSE_{NOISE} (the noise dependent MSE). (Note that the suffix is capitalized to distinguish the MSE_{FREE} and the MSE_{NOISE} in the new proposal from the MSE_{free} and the MSE_{noise} in the previous model.) Therefore, MSE_{FREE} and MSE_{NOISE} are expressed by

$$\mathrm{MSE}_{\mathrm{FREE}} = \mathrm{Tr}\left\{\left(\mathrm{I}_{\mathrm{N}} - \mathrm{WS}_{\mathrm{L}}\right)\mathrm{E}\left\{\mathbf{r}\mathbf{r}^{\mathrm{T}}\right\}\left(\mathrm{I}_{\mathrm{N}} - \mathrm{WS}_{\mathrm{L}}\right)^{\mathrm{T}}\right\}, \tag{4.15}$$

$$\mathrm{MSE}_{\mathrm{NOISE}} = \sigma^2 \sum_{\mathrm{i}=1}^{\mathrm{R}} \kappa_{\mathrm{i}}{}^2 . \tag{4.16}$$

Thus the estimated system noise variance $\hat{\sigma}_{\mathrm{W}}^2$ with a reconstruction matrix W is given by

$$\hat{\sigma}_{\mathrm{W}}^2 = \left(\mathrm{MSE} - \mathrm{MSE}_{\mathrm{FREE}}\right) \Big/ \sigma^2 \sum_{\mathrm{i}=1}^{\mathrm{R}} \kappa_{\mathrm{i}}{}^2 . \tag{4.17}$$

It is appropriate to note here what kind of reconstruction matrix W is suitable for the proposed model. The $\mathrm{MSE}_{\mathrm{FREE}}$ should not contain the system noise. Therefore, the matrix W must not contain the noise as seen from the Eq.(4.15). The regression model and the Imai-Berns model are not suitable for the matrix W because the matrices contain the sensor responses with the noise as seen from Eqs.(4.6) and (4.7). On the other hand, the reconstruction matrix of the linear model and the reconstruction matrix $\mathrm{W}(0)$ of the Wiener model are suitable for this model because they don't contain the noise in the matrices.

4.4 Experimental Procedures

A multispectral color image acquisition system was assembled by using seven interference filters (Asahi Spectral Corporation) in conjunction with a monochrome video camera (Kodak KAI-4021M). Image data from the video camera were converted to 8-bit-depth digital data by an AD converter. The spectral sensitivity of the video camera was measured over wavelengths from 400 to 700 nm at 10-nm intervals. The measured spectral sensitivities of the camera are shown in Fig.4.1. The illuminant used for the image capture was the illuminant which simulates the daylight (Seric Solax XC-100AF). The spectral power distribution of the illuminant measured by the spectroradiometer (Minolta CS-1000) is presented in Fig.4.2.

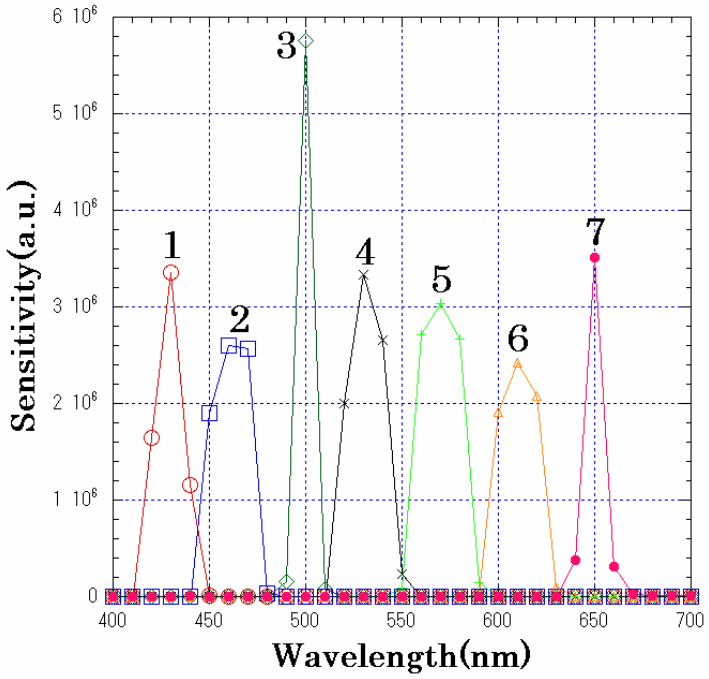

Fig. 4.1. Spectral sensitivities of each sensor.

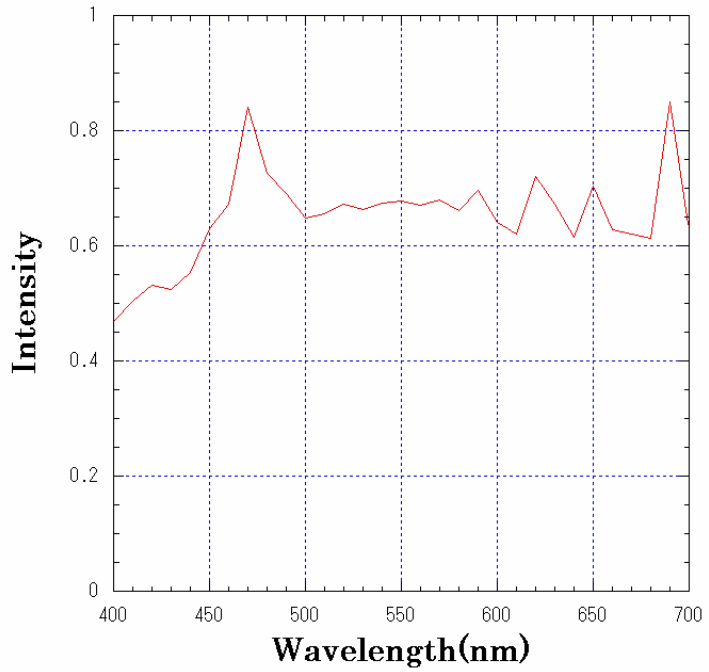

Fig. 4.2. Spectral power distribution of the recording illumination.

The GretagMacbeth ColorChecker (24 colors) was illuminated from the direction of about 45 degree to the surface normal, and the images were captured by the camera from the normal direction. The image data were corrected to uniform the nonuniformity in illumination and sensitivities of the pixels of a CCD. The computed responses from a camera to a color by using the measured spectral sensitivities of the sensors, the illuminant and the surface reflectance of the color do not equal to the actual sensor responses since the absolute spectral sensitivities of a camera depend on the camera gain. Therefore, the sensitivities were calibrated using an achromatic color in the charts. In this work, the constraint was imposed on the signal power as given by $\rho = \mathrm{Tr}\left(S_L R_{SS} S_L^T\right)$, where relation of $\rho = 1$ was used so that the estimated system noise variance can be compared for different sensor sets. Various combinations of sensors from three to seven in Fig.4.1 were used to simulate different sensor sets.

For the Wiener estimation developed in the previous model, the system noise variance was estimated by the methods described above for each combination of sensors. Then the spectral reflectances were recovered and the MSE of the recovered spectral reflectances was computed. For other models, the spectral reflectances were recovered by each model and each MSE of the recovered spectral reflectances was also computed.

4.5 Results and Discussions

In this chapter, the learning samples were the same as the test samples, i.e., the GretagMacbeth ColorChecker was used for the test samples and the learning samples.

To estimate the influence of the system noise on the recovered spectral reflectances, a measure for an increase in the MSE by the system noise is required. In the previous model which was developed based on the Wiener estimation, the increase in the MSE ($\Delta \mathrm{MSE}_{\mathrm{Wiener}}$) by the system noise is denoted as

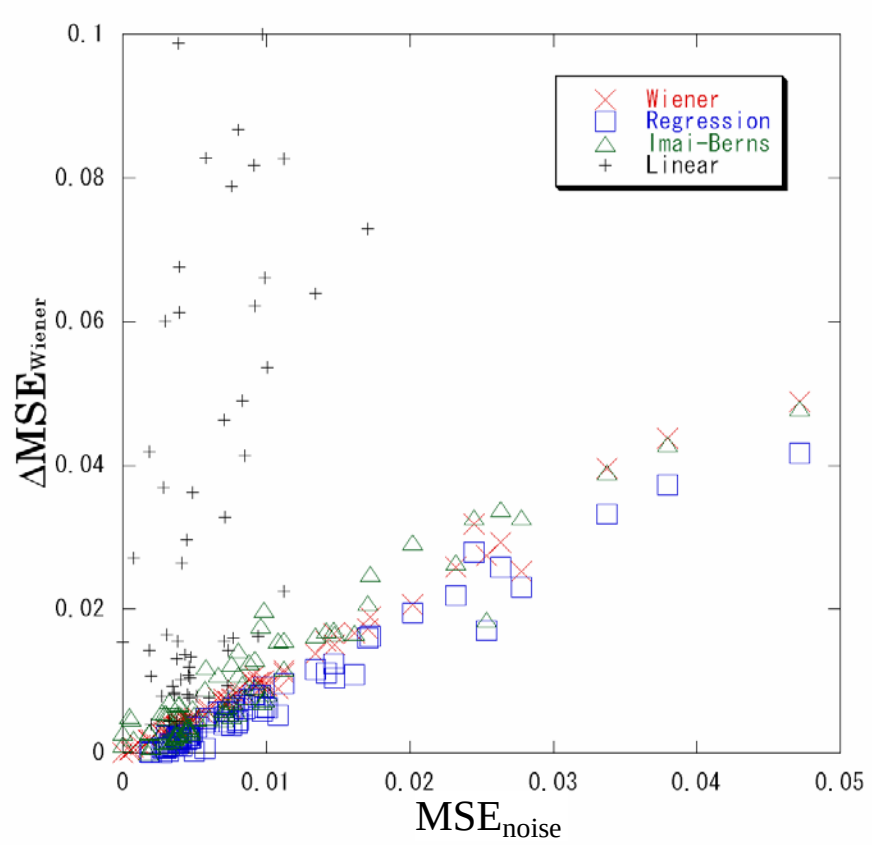

Fig. 4.3. Relation between the increase in the MSE by the noise estimated by the previous model (ΔMSE_{Wiener}) and the MSE_{noise} by the Wiener, Regression, Imai-Berns and linear model for the GretagMacbeth ColorChecker .

$$\Delta MSE_{Wiener} = MSE - MSE_{free} . \tag{4.18}$$

In the proposed model, we define the ΔMSE, which is the increase in the MSE by the system noise for each reconstruction matrix W, as

$$\Delta MSE = MSE - MSE_{FREE} . \tag{4.19}$$

The ΔMSE_{Wiener} (defined by Eq.(4.18)) as a function of MSE_{noise} for various combinations of the sensors, from three to seven sensors, for the GretagMacbeth ColorChecker are shown in Fig.4.3. For the Wiener model, the regression model and the Imai-Berns model, the ΔMSE_{Wiener} and the MSE_{noise} agree fairly well with the prediction of the previous model. This is because the multiple regression model and the Imai-Berns model are mathematically equivalent to the Wiener estimation [11,20], i.e., the matrices W_R given by Eq.(4.6) in the multiple regression model and W_I given by Eq.(4.8) in the Imai-Berns model are equivalent to the matrix $W(\sigma^2)$ in the Wiener estimation. But for the linear model the MSE_{noise} does not show good correlation to the ΔMSE_{Wiener}. The reason for this uncorrelation is considered as the MSE_{noise} is derived from the Wiener model, in which $W(\sigma^2)$ is regularized for the noise, but the reconstruction matrix $W_L = V(S_L V)^+$ by the linear model is not correctly regularized and the linear model is more sensitive to the noise compared to other reflectance reconstruction models [21].

Because the MSEnoise does not show good correlation to the ΔMSE_{Wiener} for the linear model, the relation between ΔMSE (defined by Eq.(4.19)) and $\hat{\sigma}^2 \sum_{i=1}^{R} \kappa_i^{\,2}$ (MSE_{NOISE} given by Eq.(4.16) for the linear model with the system noise variance $\hat{\sigma}^2$ estimated by the previous model, in which the κ_i is the singular value of the matrix $W_L = V(S_L V)^+$) for the linear model was studied and the results are shown in Fig.4.4(a). For the linear model, the MSE_{NOISE} agrees better than the MSE_{noise} in Fig.4.3. But it still scatters for some sets of sensors. The relation between ΔMSE (defined by Eq.(4.19)) and $\hat{\sigma}^2_{Linear} \sum_{i=1}^{R} \kappa_i^{\,2}$ (MSE_{NOISE} given by Eq.(4.16) for the linear model with the system noise variance $\hat{\sigma}^2_{Linear}$ estimated by the newly proposed model when $W = W_L$ by the Eq.(4.17)) for the linear model is shown in Fig.4.4(b). The plots agree quite well with the prediction of the proposed model. In other words, $\hat{\sigma}^2_{Linear}$ is correctly estimated by the Eq.(4.17).

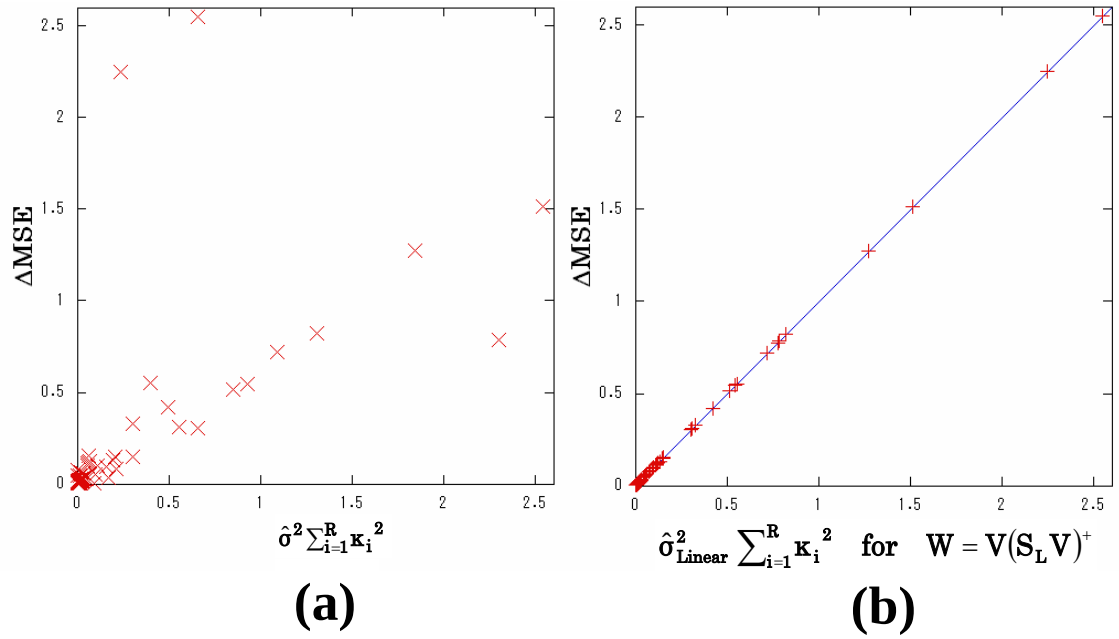

Fig. 4.4. (a) Relation between the increase in the MSE (ΔMSE) by the linear model and the MSE_{NOISE} ($\hat{\sigma}^2 \sum_{i=1}^{R} \kappa_i^2$) with the noise variance estimated with the previous model for the GretagMacbeth ColorChecker .

Fig. 4.4. (b) Relation between the increase in the MSE (ΔMSE) by the linear model and the MSE_{NOISE} ($\hat{\sigma}^2_W \sum_{i=1}^{R} \kappa_i^2$) with the noise variance estimated with the reconstruction matrix W for the GretagMacbeth ColorChecker .

It is interesting to compare the estimated system noise variance of an image acquisition device by the different models. Tbl.4.1 shows the optimum noise variance σ^2_{opt} that makes the MSE of the Wiener estimation by Eq.(4.3) minimum, which was searched by the brute force method, the estimated system noise variance $\hat{\sigma}^2$ by the previous model using Eq.(4.5) and the estimated system noise variances $\hat{\sigma}^2_{Linear}$ and $\hat{\sigma}^2_{W(0)}$ by the proposed model using Eq.(4.17), where $W = W_L$ for $\hat{\sigma}^2_{Linear}$ and $W = W(0)$ for $\hat{\sigma}^2_{W(0)}$ were used, respectively. The MSEs at each estimated system noise variance, $MSE(\sigma^2_{opt})$, $MSE(\hat{\sigma}^2)$, $MSE(\hat{\sigma}^2_{Linear})$, $MSE(\hat{\sigma}^2_{W(0)})$, are also

shown in Tbl.4.1. The MSEs larger than the corresponding minimum MSEs are indicated with bold and underlined letters. The optimum noise variance should be the true system noise variance because it makes the MSE minimum with the Wiener estimation in Eq.(4.3).

The values of estimated system noise variances $\hat{\sigma}^2$ by the previous model are similar to the optimum noise variances σ^2_{opt} and are the same as the estimated system noise variances $\hat{\sigma}^2_{W(0)}$ by the proposed model. This is because the previous model is equivalent to the proposed model when $W = W(0)$. The proof of the equivalence of the proposed model to the previous model when $W = W(0)$ is shown in the Appendix. The estimated system noise variances $\hat{\sigma}^2_{Linear}$ slightly scatter but show the same order of the magnitude to the optimum noise variances σ^2_{opt}.

Though the MSEs by the Wiener estimation with each estimated noise variance are close to the corresponding minimum MSEs, $MSE(\hat{\sigma}^2_{W(0)})$ tend to show smaller values than the $MSE(\hat{\sigma}^2_{Linear})$. It is natural that the estimated noise variance by the Wiener model fits to the Wiener model.

Although the new proposal explains the ΔMSE as a function of $\sigma^2 \sum_{i=1}^{R} \kappa_i^{\,2}$ for the linear model as shown in Fig.4.4(b), the question whether the proposal holds for the Wiener estimation is interesting. The relation between ΔMSE and MSE_{NOISE}, which is $\hat{\sigma}^2_W \sum_{i=1}^{R} \kappa_i^{\,2}$, for each model is shown in Fig.4.5, where κ_i is the i-th singular value of each reconstruction matrix W, i.e., $W = W(\hat{\sigma}^2_{W(0)})$ for the Wiener model and $W = W_L$ for the linear model are used, respectively. The $\hat{\sigma}^2_W$ represents $\hat{\sigma}^2_W = \hat{\sigma}^2_{W(0)}$ for the Wiener model and $\hat{\sigma}^2_W = \hat{\sigma}^2_{Linear}$ for the linear model. Though the plots scatter a little for the Wiener model, the formulation of the MSE_{NOISE} is also applicable to the Wiener model.

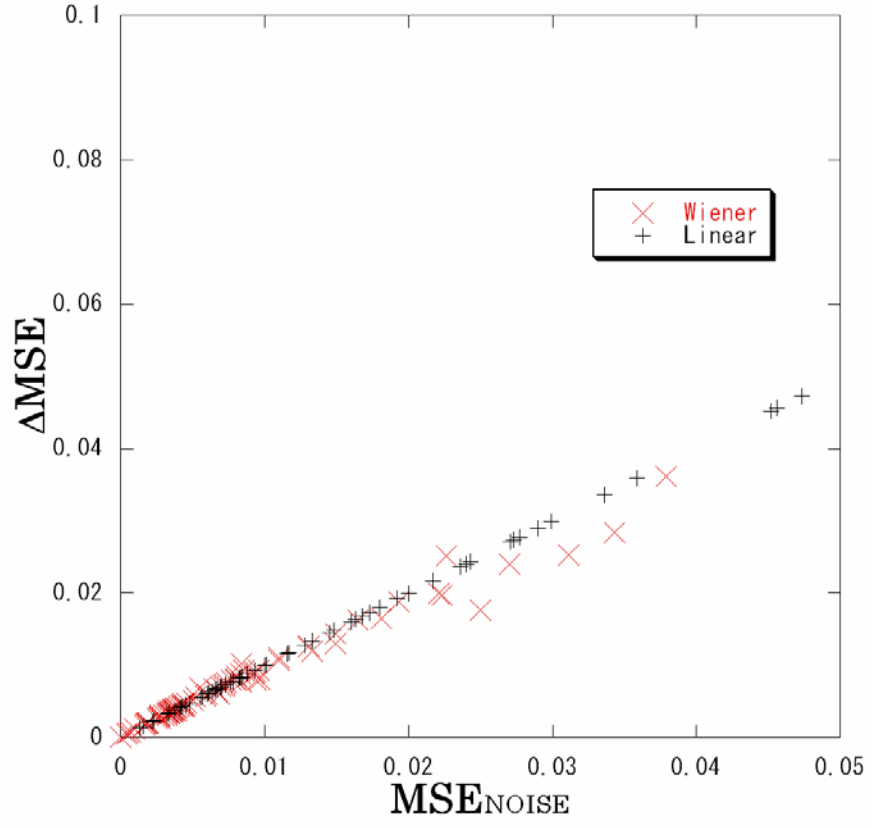

Fig. 4.5. Relation between the increase in the MSE (ΔMSE) and MSE_{NOISE} by the Wiener and the linear model.

Table 4.1. Estimated system noise variance and the MSE by the Wiener model with each estimated system noise variance.

Sensors	σ^2_{opt} [a]	$\hat{\sigma}^2$ [b]	$\hat{\sigma}^2_{Linear}$ [c]	$\hat{\sigma}^2_{W(0)}$ [d]	$MSE(\sigma^2_{opt})$ [e]	$MSE(\hat{\sigma}^2)$ [f]	$MSE(\hat{\sigma}^2_{Linear})$ [g]	$MSE(\hat{\sigma}^2_{W(0)})$ [h]
1234567	1.15E-04	8.39E-05	1.42E-04	8.39E-05	1.33E-02	1.33E-02	1.33E-02	1.33E-02
123456	1.45E-04	1.33E-04	6.55E-05	1.33E-04	4.41E-02	4.41E-02	**4.44E-02** [*]	4.41E-02
123457	1.14E-04	1.05E-04	7.06E-05	1.05E-04	1.78E-02	1.78E-02	**1.79E-02** [*]	1.78E-02
123467	1.79E-04	1.22E-04	6.78E-05	1.22E-04	1.63E-02	1.63E-02	**1.64E-02** [*]	1.63E-02
123567	1.60E-04	1.17E-04	6.99E-05	1.17E-04	1.60E-02	1.60E-02	**1.61E-02** [*]	1.60E-02
124567	1.31E-04	1.17E-04	1.26E-04	1.17E-04	1.67E-02	1.67E-02	1.67E-02	1.67E-02
134567	2.09E-04	1.20E-04	2.10E-04	1.20E-04	1.58E-02	**1.59E-02** [*]	1.58E-02	**1.59E-02** [*]
234567	1.64E-04	9.21E-05	1.83E-04	9.21E-05	1.68E-02	1.68E-02	1.68E-02	1.68E-02

[*] MSEs larger than the optimum MSE are bold.

[a] Optimum noise variance that minimizes the MSE searched by the brute force method by the Eq.(4.3).

[b] System noise variance estimated by the previous model (Eq.(4.5)).

[c] System noise variance estimated by the proposed model (Eq.(4.17)) with the matrix W_L of the linear model.

[d] System noise variance estimated by the proposed model (Eq.(4.17)) with the matrix $W(0)$ of the Wiener model by letting $\sigma_e^2 = 0$ in Eq.(4.3).

[e] Minimum MSE recovered by the Wiener model in Eq.(4.3) with $\sigma_e^2 = \sigma_{opt}^2$.

[f] MSE recovered by the Wiener model in Eq.(4.3) with $\sigma_e^2 = \hat{\sigma}^2$.

[g] MSE recovered by the Wiener model in Eq.(4.3) with $\sigma_e^2 = \hat{\sigma}^2_{Linear}$.

[h] MSE recovered by the Wiener model in Eq.(4.3) with $\sigma_e^2 = \hat{\sigma}^2_{W(0)}$.

To examine the reason for the increase in the MSE by the system noise, the relation between ΔMSE and $\sum_{i=1}^{R} \kappa_i^2$ or ΔMSE and $\hat{\sigma}_W^2$ by the Wiener and the linear model for various combinations of the sensors is shown in Fig.4.6. The plots for the estimated system noise variances lie in the nearly same order of the magnitude regardless of the increase in ΔMSE. It is very important to note that the estimated noise variance does not contribute to the increase in ΔMSE and that those estimates are nearly independent to the reconstruction models. On the other hand, the values of $\sum_{i=1}^{R} \kappa_i^2$ increase with the increase in ΔMSE for the linear model, whereas the values of $\sum_{i=1}^{R} \kappa_i^2$ remain almost constant for the Wiener model with the increase in ΔMSE. This means that the increase in $\sum_{i=1}^{R} \kappa_i^2$ causes the increase in the MSE. In other words, the system noise is amplified by $\sum_{i=1}^{R} \kappa_i^2$ as shown in Eq.(4.16) and this fact shows that the sum of the squared singular values of the reconstruction matrix of the image acquisition device should be small to design a noise robust system.

As mentioned above, the reconstruction matrices of the regression model and the Imai-Berns models are not suitable for the proposed model because their reconstruction matrices contain the system noise. Knowing this limitation, the relation between the increase in the MSE and the MSE_{NOISE} are examined. For the regression model and the Imai-Berns model, MSE_{FREE} gives inaccurate values since the reconstruction matrices W_R and W_I contain the system noise, thus another definition of the MSE_{FREE} is required for the increase in the MSE.

Let the MSE with the sensor response $\mathbf{p}$ be $MSEp(\mathbf{p})$. Let $\hat{\mathbf{p}} = SL\mathbf{r}$ then the MSE in the noiseless case is denoted as $MSEp(\hat{\mathbf{p}})$. Thus the $\Delta MSEp$, the increase in the MSE by the system noise, is defined without MSE_{FREE} as

$$\Delta MSEp = MSEp(\mathbf{p}) - MSEp(\hat{\mathbf{p}}). \tag{4.20}$$

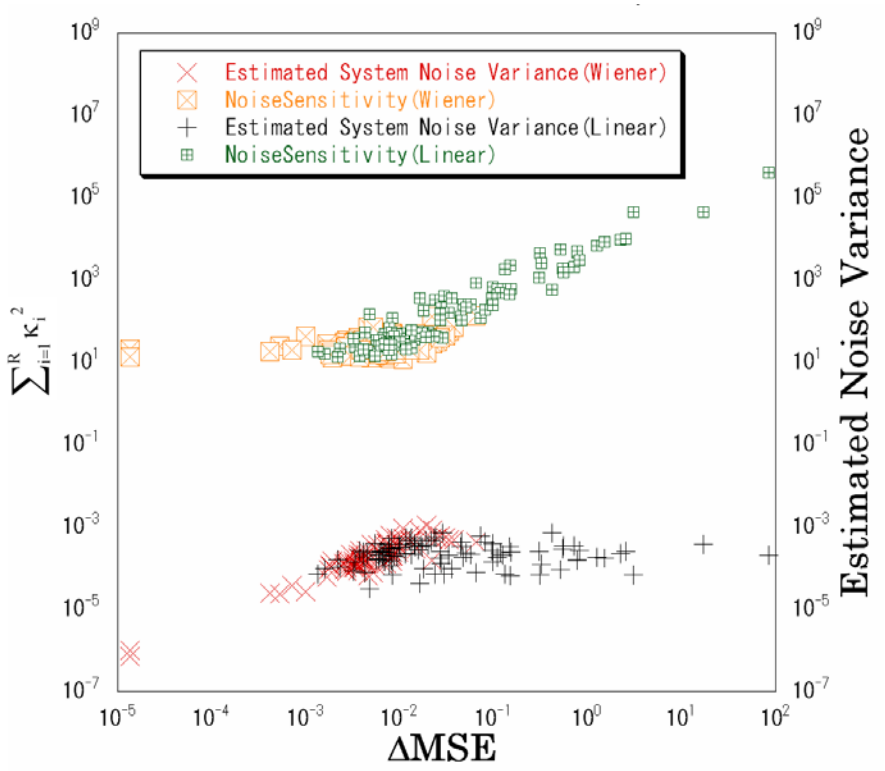

Fig. 4.6. Relation between the increase in the MSE (ΔMSE) and the Noise Sensitivity for the reconstruction matrix W ($\sum_{i=1}^{R} \kappa_i^2$) or the estimated noise variance.

In other words, ΔMSEp is the difference between the MSE calculated by the actual sensor response $\mathbf{p}$ and the MSE calculated by the noiseless sensor response $\hat{\mathbf{p}}$, i.e., $\hat{\mathbf{p}}$ is calculated from the spectral characteristics of the sensors, an illumination and a reflectance. Every reflectance recovery model calculates MSE from the sensor response thus it is now possible to define the increase in the MSE by the system noise for any recovery models.

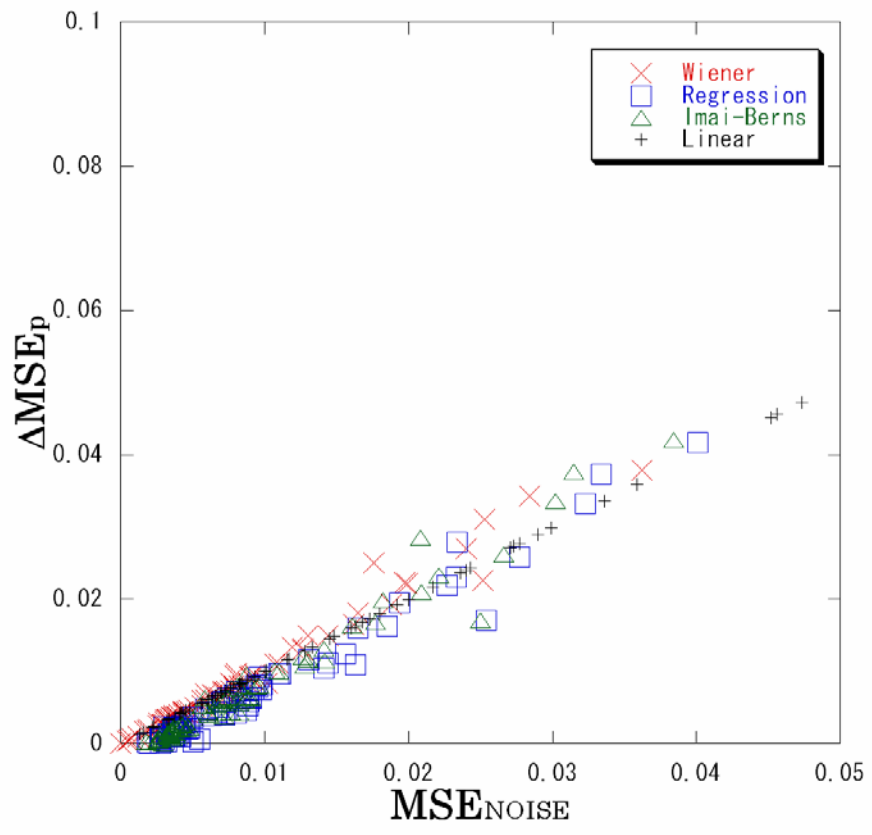

Fig. 4.7. Relation between the increase in the MSE (ΔMSEp) by the Wiener, regression, Imai-Berns and linear model and the MSE_{NOISE} ($\hat{\sigma}_W^2 \sum_{i=1}^{R} \kappa_i^{\,2}$) with the noise variance estimated with the reconstruction matrix W for the GretagMacbeth ColorChecker .

The relation between ΔMSEp and $MSE_{NOISE}= \hat{\sigma}_W^2 \sum_{i=1}^{R} \kappa_i^{\,2}$ for each model are shown in Fig.4.7, where κ_i is the i-th singular value of the matrix for each reconstruction matrix W, i.e., $W = W\left(\hat{\sigma}_{W(0)}^2\right)$ for the Wiener model , $W = W_R$ for the regression model, $W = W_I$ for the Imai-Berns model, and $W = W_L$ for the linear model, and the $\hat{\sigma}_W^2 = \hat{\sigma}_{W(0)}^2$ for the Wiener, regression, Imai-Berns model, $\hat{\sigma}_W^2 = \hat{\sigma}_{Linear}^2$ for the linear model were used. Though the plots scatter a little for the regression and the Imai-Berns model, MSE_{NOISE} shows good correlation with the

ΔMSEp for each model. The experimental results show that the proposal also holds for the regression and the Imai-Berns models.

In addition to the above mentioned estimation of the noise variance by the Wiener and the linear model, there is another method to formulate the reconstruction matrices W straight-forward by the regression or the Imai-Berns model [22] and analyze the effect of the noise to the image acquisition [23]. Further analysis to compare this straight-forward method with ΔMSEp is required to obtain more precise results.

4.6 Conclusions

A model for the influence of the noise on the accuracy of the recovered spectral reflectances is proposed and is applied to the analysis of the increase in the MSE by the system noise for the Wiener, regression, Imai-Berns and the linear model [24,25]. The experimental results by the multispectral camera agree quite well with the proposed model. From this result, it is concluded that the proposed model is appropriately formulated and that the separation of the MSE into MSE_{FREE} and the MSE_{NOISE} is essential to evaluate the influence of the system noise on the image acquisition system. The proposed model also gives an advantage to estimate the system noise variance for a reconstruction matrix W. The MSE_{NOISE} is expressed by the product of the system noise variance and the sum of the squared singular values of the matrix W. The estimated noise variances are almost independent to the matrix W and the sum of the squared singular values is largely dependent on the matrix.

References

1. H. E. J. Neugebauer, "Quality Factor for Filters Whose Spectral Transmittances are Different from Color Mixture Curves, and Its Application to Color Photography," J. Opt. Soc. Am. 46, 821-824 (1956) .
2. Poorvi L. Vora, H. Joel Trussell, "Measure of goodness of a set of color-scanning filters," J. Opt. Soc. Am. A 10, 1499-1508 (1993).
3. G. Sharma, H. J. Trussell, “Figure of merit for color scanners,” IEEE Trans. Image Process. 6, 990-1001 (1997).
4. S. Quan, N. Ohta, R. S. Berns, and X. Jiang, “Unified measure of goodness and optimal design of spectral sensitivity functions,” J. Imaging Sci. Technol. 46, 485–497 (2002).
5. N. Shimano, “Optimization of spectral sensitivities with Gaussian distribution functions for a color image acquisition device in the presence of noise,” Opt. Eng. 45, 013201 (2006).
6. G. Sharma, H. J. Trussell, and M. J. Vrhel, “Optimal nonnegative color scanning filters,” IEEE Trans. Image Process. 7, 129-133 (1998).
7. N. Shimano, “Recovery of spectral reflectances of objects being imaged without prior knowledge,” IEEE Trans. Image Process. 15, 1848-1856 (2006).
8. N. Shimano, “Suppression of noise effect in color corrections by spectral sensitivities of image sensors,” Opt. Rev. 9, 81-88(2002).
9. N. Shimano, “Application of a colorimetric evaluation model to multispectral color image acquisition systems,” J. Imaging Sci. Technol. 49, 588-593 (2005).
10. N. Shimano, “Evaluation of a multispectral image acquisition system aimed at reconstruction of spectral reflectances,” Opt. Eng. 44, 107005 (2005).
11. M. Hironaga, N. Shimano, “Evaluating the quality of an image acquisition device aimed at the reconstruction of spectral reflectances using recovery models,” J. Imaging Sci. Technol. 52, 030503 (2008).
12. M. Hironaga, N. Shimano, "Noise robustness of a colorimetric evaluation model for image acquisition devices with different characterization models," Appl. Opt. 48, 5354-5362 (2009).
13. N. Shimano, “Influence of Noise on Color Correction”, Proc. The first European Conference on Colour in Graphics, Image and Vision, 549-553 (2002).

14. M. Hironaga, N. Shimano, “Influence of Noise on Estimating Spectral Reflectances”, Proc. Color Forum Japan, 79-82 (2008).
15. Y. Zhao, L. A. Taplin, M. Nezamabadi and R. S. Berns, “Using the Matrix R Method for Spectral Image Archives”, The 10th Congress of the International Color Association (AIC’5), (Granada, Spain), pp.469-472 (2005).
16. G. H. Golub, C. F. V. Loan, [Matrix Computations], The Johns Hopkins.
17. F. H. Imai, R. S. Berns, "Spectral Estimation Using Trichromatic Digital Cameras", Proc. Int. Symposium on Multispectral Imaging and Color Reproduction for Digital Archives, Chiba, Japan. 42-49, (1999).
18. L. Maloney, "Evaluation of linear models of surface spectral reflectance with small numbers of parameters," J. Opt. Soc. Am. A **3**, 1673-1683 (1986).
19. J. Parkkinen, J. Hallikainen, and T. Jaaskelainen, "Characteristic spectra of Munsell colors," J. Opt. Soc. Am. A **6**, 318-322 (1989).
20. M. A. López-Álvarez, J. Hernández-Andrés and J. Romero, "Developing an optimum computer-designed multispectral system comprising a monochrome CCD camera and a liquid-crystal tunable filter," Appl. Opt. **47**, 4381-4390 (2008).
21. N. Shimano, K. Terai, and M. Hironaga, "Recovery of spectral reflectances of objects being imaged by multispectral cameras," J. Opt. Soc. Am. A **24**, 3211-3219 (2007).
22. M. Hironaga, N. Shimano and T. Toriu, "Estimating the Noise Variance in an Image Acquisition System with Multiple Reconstruction Matrixes", ICIC Express Letters, Vol. 6, No. 5, 1169-1174 (2012).
23. M. Hironaga, N. Shimano, T. Toriu, "Evaluating the Noise Variance of an Image Acquisition System with Various Reconstruction Matrices", CGIV 2012,6th European Conference on Colour in Graphics, Imaging 247-252, Amsterdam, the Netherlands (2012).
24. M. Hironaga, N. Shimano, "Estimating the noise influence on recovering reflectances", Proc. SPIE, Vol.7529, 75290M, San Jose, California, USA (2010).
25. M. Hironaga and N. Shimano, "Estimating the noise variance in an image acquisition system and its influence on the accuracy of recovered spectral reflectances," Appl. Opt. 49, 6140-6148 (2010).

Appendix

Proof of the equivalence of the proposed model to the previous model where $W = W(0)$.

As given by Eq.(4.13), the MSE of the recovered spectral reflectances by a matrix W is expressed by

$$\mathrm{MSE} = \mathrm{Tr}\left\{(I_N - WS_L)E\left\{\mathbf{r}\mathbf{r}^T\right\}(I_N - WS_L)^T\right\} + \sigma^2 \mathrm{Tr}\left(W^T W\right). \tag{A4.1}$$

The matrix $W(0)$ for the Wiener estimation with $\sigma_e^2 = 0$ is represented by letting $\sigma_e^2 = 0$ in Eq.(4.3) as

$$W(0) = \mathrm{Rss}S_L^T\left(S_L \mathrm{Rss} S_L^T\right)^{-1}. \tag{A4.2}$$

Substitution of (A4.2) into (A4.1) leads the MSE at $\sigma_e^2 = 0$ to

$$\mathrm{MSE}(0) = \sum_{i=1}^{N} \lambda_i - \mathrm{Tr}\left\{\mathrm{Rss}S_L^T\left(S_L \mathrm{Rss} S_L^T\right)^{-1} S_L \mathrm{Rss}\right\} + \sigma^2 \mathrm{Tr}\left(W^T W\right), \tag{A4.3}$$

where the relations such as $E\left\{\mathbf{r}\mathbf{r}^T\right\} = \mathrm{Rss}$, $\mathrm{Tr}(\mathrm{Rss}) = \sum_{i=1}^{N} \lambda_i$, and $\mathrm{Tr}\left\{\mathrm{Rss}S_L^T\left(\left(S_L \mathrm{Rss} S_L^T\right)^{-1}\right)^T S_L \mathrm{Rss}\right\} = \mathrm{Tr}\left\{\mathrm{Rss}S_L^T\left(S_L \mathrm{Rss} S_L^T\right)^{-1} S_L \mathrm{Rss}\right\}$ were used to derive (A4.3).

SVD of $S_L V \Lambda^{1/2}$ in Eq.(A4.3) leads to the previous formula Eq.(4.5),i.e.,

$$\mathrm{MSE}(0) = \sum_{i=1}^{N} \lambda_i - \sum_{i=1}^{N}\sum_{j=1}^{R} \lambda_i b_{ij}^2 + \sigma^2 \sum_{i=1}^{N}\sum_{j=1}^{R} \frac{\lambda_i b_{ij}^2}{\kappa_j^{v\,2}}. \tag{A4.4}$$

On the other hand, in the new proposal, SVD of the matrix of (A4.2), $W(0)$, is directly performed. By combining Eqs.(4.14),(4.15) and (4.16), the MSE at $\sigma_e^2 = 0$, i.e., $\mathrm{MSE}(0)$ is expressed from (A4.1) as

$$\mathrm{MSE}(0) = \mathrm{Tr}\left\{(I_N - W(0)S_L)E\left\{\mathbf{r}\mathbf{r}^T\right\}(I_N - W(0)S_L)^T\right\} + \sigma^2 \sum_{i=1}^{R} \kappa_i^{\,2}. \tag{A4.5}$$

As seen Eqs.(A4.4) and (A4.5), $\mathrm{MSE}(0)$ is expressed differently, depending only on the difference of the SVD, and the $\mathrm{MSE}(0)$ is divided into the noise independent first term and the noise dependent second term. Therefore, these noise-independent terms and noise-dependent terms are equivalent in Eqs. (A4.4) and (A4.5), respectively.. The estimate of σ^2 gives the same value since the both equations are derived from (A4.1).

The equivalence of the second term in Eqs.(A4.4) and (A4.5) gives the next relation.

$$\sum_{j=1}^{R} \kappa_j^{\,2} = \sum_{j=1}^{R} \sum_{i=1}^{N} \lambda_i b_{ij}^2 \Big/ \kappa_j^{v\,2} \,. \tag{A4.6}$$

Therefore, the singular values in the previous model and the new proposal have the next relation.

$$\kappa_j^{\,2} = \sum_{i=1}^{N} \lambda_i b_{ij}^2 \Big/ \kappa_j^{v\,2} \,. \tag{A4.6}$$

As seen from the Eq.(4.4), if $\kappa_j^{v\,2} << \sigma^2$ then the $\mathrm{MSE}_{\mathrm{NOISE}}$ becomes dominant, which means that $\kappa_j^{\,2}$ increases with the decrease in $\kappa_j^{v\,2}$.

Chapter 5

Overall Conclusions

In this chapter, the overall conclusions of the research for recovering the spectral reflectances of objects being imaged by an image acquisition system are presented. The proposed method and experiments done in each chapter of this thesis are summarized and the future works are also discussed here.

To reproduce and recognize colors under the influence of the illuminants, the recovery of the reflectances of the objects being imaged is required. The recovery is generally an inverse problem and is largely affected by the noise in the image acquisition device. Because the Wiener estimation is effective for solving inverse problems, accurate estimation of the noise variance in the image acquisition system is required for accurate estimation of the reflectances by the Wiener estimation. On the other hand, every image acquisition device has a different character; some image acquisition devices are robust and insensitive to the noise while others are not robust and sensitive to the noise. To design robust image acquisition devices to recover accurate reflectances of objects and reproduce accurate colors, a method to evaluate the image acquisition device is required.

This thesis addressed the following topics with experimental results and mathematical proofs. In chapter 2, the spectral evaluation model based on the Wiener model proposed by Shimano was applied to the regression and the Imai-Berns models and it was confirmed that the proposed model can be applied to different models. In chapter 3, it was confirmed that the colorimetric evaluation model based on the Wiener model proposed by Shimano can be applied to the regression and the Imai-Berns models. And the noise robustness of the evaluation model was examined and it was confirmed from the experimental results that the proposed model holds even in a noisy condition. In chapter 4, the noise estimation model based on the Wiener estimation proposed by Shimano was extended to a comprehensive model with a reconstruction matrix W and the mean square errors (MSE) between the recovered spectral reflectances with various reconstruction matrices W and actual spectral reflectances are divided into the noise independent MSE (MSE_{FREE}) and the noise dependent MSE (MSE_{NOISE}). It was shown that the relation between the increase in the MSE and the MSE_{NOISE} agrees quite well in the experimental results

by the multispectral camera and that the estimated noise variances are in the same order of the magnitude when the matrix W is of the Wiener model or of the linear model.

This thesis mainly addressed the influence of the noise to the image acquisition devices. For more accurate recovery of the reflectances, the choice of the learning samples is important. We tried to build a model to choose the appropriate learning sample for accurate recovery of the reflectances and some experiments are done to confirm the model but further study is required to improve the accuracy of the recovery. At the same time, an application to be used in business, out of laboratory, in much noisier environment should be developed to show the usefulness and trustworthiness of the proposed model.

Acknowledgements

First and foremost, I would like to express my indebtedness and deepest sense of gratitude to my reverend supervisor and mentor Professor Takashi Toriu, Graduate School of Engineering, Osaka City University, for his competent guidance, continuous encouragement, everlasting understanding, and strong support on numerous occasions throughout the entire phase of my research work.

I would like to express my immense sense of gratitude to the member of my thesis committee, Professor Ikuo Oka, Graduate School of Engineering, Osaka City University, for his helpful suggestions. His benevolent inspiration and kind observation motivated me to perform this novel task.

I owe the immense measure of gratitude to the member of my thesis committee, Professor Hideya Takahashi, Graduate School of Engineering, Osaka City University, for his generously responsive suggestions help me to write this thesis nicely.

I wish to express my gratitude to Professor Noriyuki Shimano, Graduate School of Science and Engineering, Kinki University, for his thoughtful suggestions and constructive discussions. I have been honored to share his superlative experience in the field of the multispectral color science.

Finally, I would like to express my special thanks to retired Professor Sadahiko Nagae, Kinki University, and retired Professor Takuya Nishimura, Kinki University, for introducing me to a rich and beautiful area of research and for sharing with me their incredibly broad knowledge.

List of Publications

Journal Papers

1. M. Hironaga, N. Shimano, "Evaluating the quality of an image acquisition device aimed at the reconstruction of spectral reflectances using recovery models," J. Imag. Sci. Technol. 52, 030503(2008).
2. M. Hironaga, N. Shimano, "Noise robustness of a colorimetric evaluation model for image acquisition devices with different characterization models," Appl. Opt. 48, 5354-5362 (2009).
3. M. Hironaga and N. Shimano, "Estimating the noise variance in an image acquisition system and its influence on the accuracy of recovered spectral reflectances," Appl. Opt. 49, 6140-6148 (2010).
4. M. Hironaga, N. Shimano and T. Toriu, "Estimating the Noise Variance in an Image Acquisition System with Multiple Reconstruction Matrixes", ICIC Express Letters, Vol. 6, No. 5, 1169-1174 (2012).
5. N. Shimano, K. Terai, and M. Hironaga, "Recovery of spectral reflectances of objects being imaged by multispectral cameras," J. Opt. Soc. Am. A 24, 3211-3219 (2007).
6. N. Shimano and M. Hironaga, "Recovery of spectral reflectances of imaged objects by the use of features of spectral reflectances," J. Opt. Soc. Am. A 27, 251-258 (2010).

Refereed Conference Proceedings

1. M. Hironaga, K. Terai and N. Shimano, "A model to evaluate color image acquisition systems aimed at the reconstruction of spectral reflectances", Proc. 9th Int. Symposium on Multispectral Color Sci. and Appl., Taipei, ROC 23-28 (2007)
2. N. Shimano, M. Hironaga, "Analysis of Mean Square Errors of Spectral Reflectances Recovered by Multispectral Cameras", Proc. of 15th Color Image Conference 147-150 Albuquerque, USA (2007)
3. M. Hironaga, N. Shimano, "Colorimetric Evaluation of a Set of Spectral Sensitivities", CGIV 2008, 4th European Conference on Colour in Graphics, Imaging, and MCS/08 602-607, Terrassa, Spain (2008)
4. N. Shimano, M. Hironaga, "A new proposal for the accurate recovery of spectral reflectances of imaged objects without prior knowledge", Proc. of Archiving 2008 pp. 155-158, IS&T, Bern, Switzerland (2008)
5. N. Shimano, M. Hironaga, "Adaptive Recovery of Spectral Reflectances by the Regularized Wiener Filter",11th Congress of the International Colour Association Sydney, Australia (2009)
6. M. Hironaga, N. Shimano, "Estimating the noise influence on recovering reflectances", Proc. SPIE, Vol.7529, 75290M, San Jose, California, USA (2010)
7. M. Hironaga, N. Shimano, T. Toriu, "Evaluating the Noise Variance of an Image Acquisition System with Various Reconstruction Matrices", CGIV 2012,6th European Conference on Colour in Graphics, Imaging 247-252, Amsterdam, the Netherlands (2012)